Simvastatin Encapsulation in Alginate-Based Microspheres

Ava Parsian

A thesis submitted to the Faculty of Graduate and Postdoctoral Studies
in partial fulfillment of the requirements for the degree of

MASTER OF APPLIED SCIENCE

in Biomedical Engineering

Ottawa-Carleton Institute for Biomedical Engineering
University of Ottawa, Ottawa, Ontario, Canada

March 2016

Acknowledgements

First and foremost, I offer my profoundest gratitude to my thesis supervisor, Dr. Isabelle Catelas, for her expertise and ongoing support and guidance for the completion of this thesis. I am also grateful for her valuable dedication to my professional development outside of the lab, which has made my graduate experience one that I will forever cherish.

I would like to thank my committee members, Dr. Marianne Fenech (Mechanical Engineering), and Dr. Xudong Cao (Chemical and Biological Engineering) for dedicating their time and energy in reviewing my thesis. I would also like to thank the members of Orthopaedic Bioengineering Laboratory (Dr. Catelas' lab), especially Dr. Eric A. Lehoux, Research Associate in the lab, who was always willing to help and provide his best advice on my research experiments. I cannot thank him enough for his kindness and words of encouragement. My heartfelt thanks go to my fellow wonderful lab-mates, Stephen J. Baskey, Zeina Salloum and Maxime-Alexandre Ferko for their energy and support, which provided such a positive and joyous atmosphere in the lab. Because of them all, I always looked forward to coming to the lab every day.

Last but not least, I would like to express my sincere gratitude to my parents and brother for their unflagging love, support and strength throughout this journey. I am forever indebted to them for all the sacrifices that they have made for me so that I could pursue my dreams.

Thesis Organization

This thesis is divided into four main Chapters and includes one manuscript.

Chapter 1 introduces the context of the work.

Chapter 2 describes the hypotheses and objectives of this thesis.

Chapter 3 is the literature review focusing on the hip joint; hip joint replacements; causes of long-term hip implant failure; biological mechanisms involved in implant wear-mediated osteolysis; anti-inflammatory agents (in particular simvastatin) for the treatment of aseptic loosening; local and controlled delivery of simvastatin; 2-hydroxypropyl-β-cyclodextrin as a water-soluble drug excipient to increase simvastatin solubility; and finally alginate polymer for drug delivery.

Chapter 4 is the manuscript, to be submitted to the Journal of Biomedical Materials Research Part B: Applied Biomaterials. It focuses on approaches to maximize simvastatin encapsulation in alginate-based microspheres. More specifically, it describes the complexation of simvastatin with 2-hydroxypropyl-β-cyclodextrin to increase its solubility in alginate solution, as well as the effects of chitosan and dextran sulfate on simvastatin encapsulation efficiency. The effects of gelation conditions (volume of the gelation medium, curing time, and addition of simvastatin in the gelation medium) were also studied. The size and morphological analysis of the simvastatin-loaded alginate-based microspheres with the polymer formulation and gelation conditions that gave the highest simvastatin encapsulation efficiency are also included.

Chapter 5 is the overall thesis discussion, which includes the conclusions, technical considerations, and future studies.

Abstract

Despite the great success of hip implant surgeries, wear particle-induced implant aseptic loosening still limits the implant longevity. Simvastatin, an FDA-approved cholesterol lowering statin, is a promising drug candidate for the treatment of implant aseptic loosening due to its anti-inflammatory properties as well as its ability to stimulate bone growth and inhibit bone resorption. In addition, alginate microspheres have been used extensively in drug delivery applications because of alginate properties, including biocompatibility and gelation in mild conditions. However, the hydrophobicity of simvastatin, as well as the large alginate microsphere pore size leading to the leakage of low molecular weight drugs are limiting factors for their use as a delivery system for simvastatin. Therefore, the objectives of this thesis were twofold: 1. To complex simvastatin with 2-hydroxypropyl-β-cyclodextrin (HP-βCD) in order to increase its solubility; and 2. To increase simvastatin encapsulation efficiency in alginate microspheres by coating the microspheres with chitosan, adding dextran sulfate in the alginate solution, and optimizing the gelation conditions used for the synthesis of the microspheres (e.g., volume of gelation medium, curing time, and addition of simvastatin in the gelation medium). Results showed that simvastatin complexation with HP-βCD increased with HP-βCD to simvastatin molar ratio, to a maximum of 97.6% at the molar ratio of 10. Results also showed that chitosan coating of the alginate microspheres increased simvastatin encapsulation efficiency (up to 10.6%), which was further improved (up to 14.0%) when adding 2.0% (w/v) dextran sulfate to the alginate solution. This increase was likely due to electrostatic interactions between dextran sulfate and chitosan in addition to alginate, resulting in a denser coating. Finally, the addition of simvastatin in the gelation medium was shown to also increase simvastatin encapsulation (up to 22.4%), likely because of a decrease in the diffusion of simvastatin out of the microspheres. Overall, this work completed the initial steps for the development of an alginate-based drug delivery system for simvastatin with the long-term goal of providing a local delivery of simvastatin to modulate implant aseptic loosening.

Table of Contents

List of Figures

List of Tables

List of Acronyms

Term	Abbreviation
2-hydroxylpropyl-β-cyclodextrin	HP-βCD
3-hydroxy-3-methylglutaryl coenzyme A	HMG-CoA
α-L-guluronic acid	G
β-cyclodextrin	β-CD
β-D-mannuronic acid	M
adipic acid dihydrazide	ADH
beta-tricalcium phosphate	β-TCP
Canadian Joint Registry Report	CJRR
ceramic-on-ceramic	CC
ceramic-on-metal	CM
ceramic-on-polyethylene	CPE
cyclooxygenase	COX
Food and Drug Administration	FDA
Gastrointestinal	GI
interleukin	IL
macrophage colony-stimulating factor	M-CSF
metal-on-metal	MM
metal-on-polyethylene	MPE
poly(lactic-co-glycolic acid)	PLGA
poly(lactic-co-glycolic acid)/hydroxyapatite	PLGA/HAp
poly(vinyl) chloride	PVC
prostaglandin E2	PGE2
receptor activator of nuclear factor κB ligand	RANKL
simulated body fluid	SBF
surface replacement	SR
three dimensional	3D
total hip replacement	THR
tumor necrosis factor-alpha	TNF-α
ultra high molecular weight polyethylene	UHWMPE

1 Introduction

Hip arthroplasties are very efficient at restoring hip function and alleviating pain in patients with end-stage arthritic diseases such as osteoarthritis and rheumatoid arthritis [1]. More than 800,000 hip arthroplasties are performed worldwide annually [2], out of which more than 31,000 are performed in Canada [3]. The overall success rate of hip replacement surgeries after 10-15 years of implantation is reported to be over 90% [4]. However, despite the great success of these implants, several physical/mechanical and biological factors still limit the implant longevity [4].

The main cause for long-term hip implant failures is aseptic loosening (i.e., the loosening of the implant in the absence of an infection), which accounts for more than 75% of the implant failures [5]. Wear particles, primarily generated from wear of the implant bearing surfaces, accumulate in the periprosthetic tissues and induce an inflammatory response, which can eventually lead to osteolysis around the implant, followed by aseptic loosening [6]. Indeed, wear particles, which are phagocytozed predominantly by macrophages, lead to the release of pro-inflammatory cytokines, such as tumour necrosis factor-α (TNF-α) [6]. These inflammatory mediators play an important role in increasing the differentiation, maturation, and activation of osteoclasts (cells responsible for resorbing bone), and in decreasing the activity of osteoblasts (cells responsible for forming new bone) [7]. Because the inflammatory response is by far the most common long-term post-surgery complication [4], it is critical to better understand and regulate the mechanisms involved in this overall response to increase implant longevity.

Simvastatin, a potent FDA-approved cholesterol-lowering statin, was shown to have properties that could be beneficial to patients with joint replacements [8]–[12]. More specifically, previous studies have demonstrated that simvastatin can decrease the inflammatory response [9], [12], stimulate bone growth [8], and decrease bone loss [10], [11]. Therefore, simvastatin appears to have effects that could counteract the biological mechanisms leading to implant loosening.

Simvastatin is currently approved for oral administration (in the form of tablets) [13]. However, in order to use simvastatin in the context of periprosthetic osteolysis modulation, a local delivery system needs to be developed to eliminate adverse side effects such as hepatic

toxicity and myopathy including rhabdomyolysis, which have been generally associated with the long-term and systemic administration of high doses of statins [14].

Alginate microspheres have attracted much interest for drug delivery applications because of alginate biocompatibility, low toxicity, relatively low cost, and mild gelation conditions [15], [16]. Alginate microspheres can be synthesized via the external gelation method, in which the alginate solution is extruded drop-wise into an ionic cross-linking solution containing divalent cations (i.e., Ca^{2+}). This results in the formation of tightly held junctions between the guluronate blocks of adjacent alginate chains, leading to a gel structure (known as egg-box structures) [15]. This cross-linking process is simple, inexpensive, and can be easily scaled up with no need for any specialized equipment [15]. More importantly, it is carried out under mild gelation conditions, which is advantageous for the encapsulation of bioactive macromolecules such as of proteins and enzymes, as well as cells [17]. Furthermore, the remarkably slow degradation rate of the cross-linked alginate (from months to years) allows prolonged drug delivery [18]–[20]. Therefore, the overall objective of this thesis was to develop an alginate-based drug delivery system for simvastatin, with the long-term goal of providing a local and sustained delivery of simvastatin in periprosthetic tissues.

2 Thesis Hypotheses and Objectives

Despite the advantages of alginate microspheres as previously described, they present some limitations for the encapsulation of hydrophobic and low molecular weight drugs (including simvastatin) because of the hydrophilic nature of the polymer [21] and the large pore size of alginate microspheres, respectively, resulting in the drug leakage during the microsphere synthesis process [22], [23]. Therefore, the overall goal of this project was to develop new alginate-based microspheres as a delivery system for simvastatin that would overcome the aforementioned limitations.

2.1 Hypotheses

1. The complexation of simvastatin with 2-hydroxypropyl-β-cyclodextrin (HP-βCD), a water-soluble drug excipient, will increase the solubility of simvastatin; and
2. Chitosan-coating of the microspheres, the addition of dextran sulfate in the alginate solution, and optimized gelation conditions will improve the encapsulation efficiency of simvastatin in alginate microspheres.

2.2 Objectives

1. To complex simvastatin with HP-βCD in order to increase its solubility; and
2. To increase simvastatin encapsulation efficiency in alginate microspheres by coating the microspheres with chitosan, adding dextran sulfate in the alginate solution, and optimizing the gelation conditions used for the synthesis of the microspheres (e.g., volume of gelation medium, curing time, and addition of simvastatin in the gelation medium).

3 Literature Review

3.1 Hip Joint

3.1.1 Hip anatomy

The hip joint is a deep enarthrodial joint at the juncture of the legs and pelvis, responsible for providing a wide range of locomotion as well as support to the human body [24]. It is known as one of the most free-moving joints and the second largest weight bearing joint in the body (after the knee joint) [24]. The hip joint is composed of the convex head of the femur (thigh bone) known as the ball, which is secured into the concave bony socket of the pelvis called the acetabulum (Figure 3.1). The ball of the femur and the acetabulum are connected via a complex system of ligaments, which provide strength and stability to the joint. A durable layer of articular cartilage covers the surfaces of the femoral head and the acetabulum, allowing for the smooth movement of the bones during loading by providing an extremely low coefficient of friction between the two bones [25].

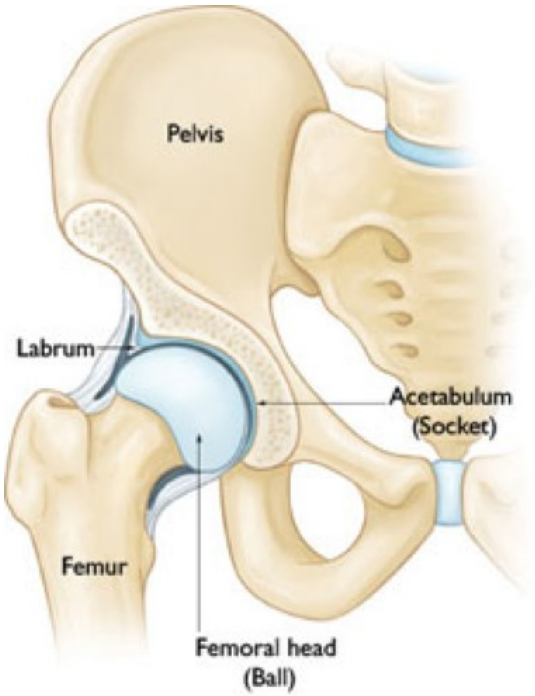

Figure 3.1 The anatomy of hip joint [26]. Reproduced with permission from Orthoinfo. ©American Academy of Orthopaedic Surgeons.

In addition, the circumferential ring of the acetabulum is covered by a strong fibrocartilage called labrum, which not only seals and surrounds the hip joint but also keeps a natural, viscous fluid called synovial fluid inside the cavity of the hip joint [25]. The synovial fluid, produced by the synovial membrane (a soft connective tissue lining the cavities of joints), provides nutrition to the articular cartilage and functions as a lubricant to reduce friction between the bones. It also works as the 'shock absorber' in the joint by taking some of the load off the bones via fluid pressurization [27].

3.1.2 Hip-related diseases

Hip-related diseases are primarily caused by various forms of degenerative arthritis and related disorders that can affect the bone and/or muscles of the hip joint. According to the Canadian Joint Registry Report (CJRR), degenerative osteoarthritis is the most prevalent cause of the hip joint damage [3], affecting more than three million Canadians [28].

Osteoarthritis occurs over time due to the erosion of the hyaline articular cartilage covering the femoral head and the acetabulum. The loss of cartilage leads to the direct bone-on-bone movement with increased resistance, which may also stimulate growths of bone (called spurs) around the joint, resulting in a severe pain, stiffness, and swelling in the affected joint [29]. Other factors causing the break-down of the cartilage in the hip joint include a fracture or similar injury to the hip bone resulting from high load or trauma, rheumatoid arthritis, lupus (the latter two being chronic autoimmune disorders causing the inflammation of the joint), or infectious arthritis, also called septic arthritis (caused by bacterial, viral or fungi infections in the blood) [30]. In younger patients, juvenile arthritis (arthritis beginning before the age of 16) and femoroacetabular impingement (abnormal anatomy of the hip joint) cause the premature cartilage deterioration, leading to early hip dysfunction [31].

Despite being an age-related disorder, not everyone develops osteoarthritis. Indeed, several factors such as genetics, gender (higher prevalence in women above 55 years), nutrition (uptake of vitamins C, D and E), life style (obesity and levels of exercise), and bone density contribute to the onset of the disease [32]. Nevertheless, with the aging population, the debilitating effects of this disorder pose an increased financial burden on the health care [33], [34].

3.1.3 Non-operative hip disease treatments

The first line of treatments to reduce pain and increase mobility is a combination of non-operative measurements such as anti-inflammatory drugs (discussed in Section 3.5) which are given to patients by primary care physicians [35]. However, if the non-operative treatments are not effective in easing the pain and symptoms, a surgical intervention is considered [36].

3.2 Hip Joint Replacements

According to the CJRR, the most common diagnosis for hip replacements was reported to be degenerative osteoarthritis, acute hip fracture, and osteonecrosis (82.1%, 6.3% and 3.5%, respectively) [3].

A hip joint replacement is very efficient at restoring joint function and alleviating pain in patients with end-stage arthritis. It is performed by surgical removal of the bone and cartilage of the diseased hip joint followed by their replacement with hip implants [37]. The modern hip implant is composed of a ball-and-socket structure, which mimics the function of the biological joint by allowing the femur to circumduct freely in a 360-degree motion. Hip implants can be either total hip replacements (THR) with a stem introduced in the femur, or surface replacements (SR). Although the THR terminology sometimes also refers to a SR, THR will be exclusively used in the context of stem-type device in the present thesis.

The THR are made of three components: a femoral stem that is inserted into the femur; a femoral head (or ball) attached to the top of the femoral stem; and an acetabular component (or cup) that is inserted in the pelvis [2]. On the other hand, the SR is a bone-conserving method in which the natural femoral head and neck are not surgically removed and instead, the joint articular surfaces are replaced with a smooth metal covering [38]. Figure 3.2 shows a drawing of a SR and a THR.

According to the CJRR, 31,666 THR, 817 SR, and 10,230 partial hip replacement surgeries were performed in Canada in 2010-2011, representing an increase of 10.6% since 2006-2007 [3]. The demand for hip replacements is expected to increase [39], as the population of the baby boomer increases and as the age of the patients requiring implants decreases [40]. Indeed, amongst the 42,713 hip surgeries reported by the CJRR in 2010-2011, 5319 of them were performed in individuals less than 55 years old [3].

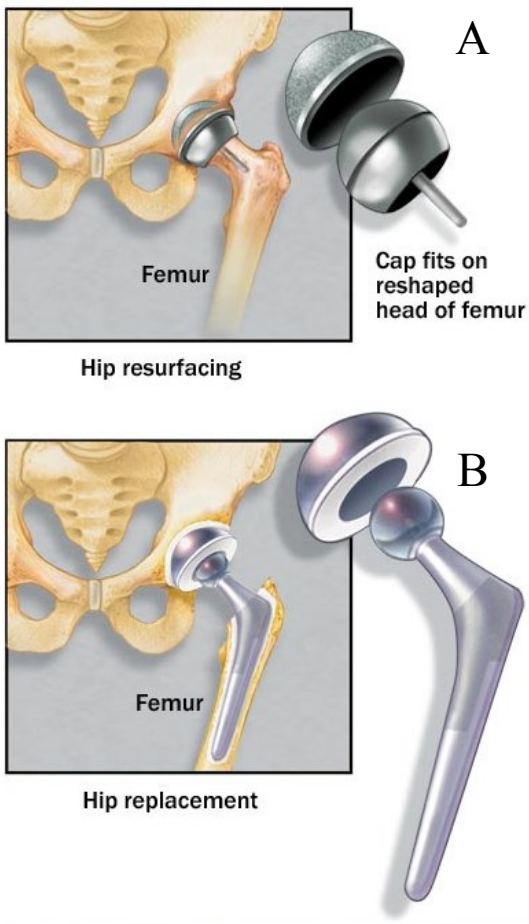

Figure 3.2 An illustration of (A) a hip surface replacement (hip resurfacing) and (B) a total hip replacement [41]. Used with permission of Mayo Foundation for Medical Education and Research. All rights reserved.

The bearing surfaces of the modern implants are composed of a combination of materials including metals, polyethylene, and ceramics. More specifically, available implant bearings include metal-on-polyethylene (MPE), metal-on-metal (MM), ceramic-on-ceramic (CC), ceramic-on-polyethylene (CPE), and ceramic-on-metal (CM). According to the CJRR, the most common bearing surfaces used in 2010-2011 were MPE (75.2%), followed by MM (10.1%), CC (9.4%) and CPE (5.3%), although MM implants have seen a decline in the last few years because of an increasing number of adverse tissue reactions reported early on with some MM hip implants. Within the MPE category, highly cross-linked polyethylene was predominantly used in the procedures (68.6%) compared to the standard ultra high molecular weight polyethylene (UHMWPE) (6.6%) [3].

Each of these surface bearings has its own advantages and disadvantages based on the characteristics of the materials. For instance, one advantage of MM hip implants is their low volumetric wear compared to conventional MPE [42]. However, the higher levels of metal ions observed with MM implants is a cause of concern as ions have been associated with adverse tissue reactions [43]–[45]. Nevertheless, continuing efforts are being made to optimize the implant design and to develop new bearing materials in order to enhance the quality of the implants and increase their longevity, thereby improving the patients' quality of life.

3.3 Causes of Long-Term Hip Implant Failure

Follow-up studies on patients with a hip implant have reported an overall success rate of over 90% after 10-15 years of implantation [4]. However, despite the great success of the implants, there are still several mechanisms of failure that limit their longevity. Indeed, there is a combination of physical/mechanical and biological factors that lead to the need of revision surgery [4]. The main cause for hip implant failures is the long-term aseptic loosening, which accounts for more than 75% of the failures [7], while infection is responsible for 7% of the revision surgeries, followed by recurrent dislocation (6%), periprosthetic fracture (5%), and surgical error (3%) [1].

Aseptic loosening of the implant is a debilitating condition, in which the bone recedes from the implant, resulting in the 'loosening' of the implant [46]. It is commonly manifested as pain and eventually shows on post-operative follow-up radiographs (as illustrated by Figure 3.3). Unfortunately, because of the slow progress of bone destruction around the implant, the signs may not be clinically detectable on radiographs until the severity of the pain and the subsequent disability require a revision surgery [46].

While the causes of aseptic loosening are reported to be multifactorial, including mechanical factors, the inflammatory response to the implant wear particles leading to periprosthetic osteolysis has been recognized to play a major role [5], [6], [46], [47]. In the 1970s, aseptic loosening was perceived to be associated with the body reaction to wear particles of cement, which was used to fix the implant into the bone, and was referred to as the 'bone cement disease' [48]. However, in the following years, the analysis of the aseptic loosening in cement-free hip implants with the presence of the implant wear particles in periprosthetic tissues

has led to a change of the term for 'wear-mediated osteolysis'. The wear particle-induced osteolysis has now been associated with every available types of implant bearings in use [49].

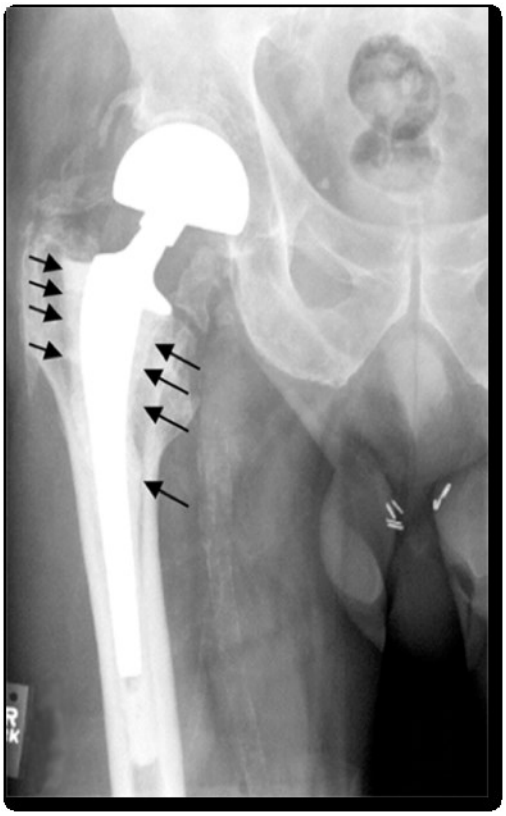

Figure 3.3 X-ray image depicting osteolysis (arrows) around a hip implant [50]. Reproduced with permission from BioMed Central Ltd.

3.4 Biological Mechanisms Involved in Implant Wear-Mediated Osteolysis

Wear particles primarily generated from the wear of the implant bearing surfaces (including metal, polyethylene and ceramics) and metal ions released from the implant metal components are known to be largely involved in the periprosthetic osteolysis leading to aseptic loosening [51]–[54].

Wear particles are primarily released when the articulating surfaces of the implant components move against each other under loading [55]–[57]. The majority of polyethylene wear particles have been reported to be in the submicron range, with an average size of about 0.5-1 μm [58], [59], whereas ceramic wear particles have been shown to present a bimodal size distribution including 5-25 nm (under normal wear condition) and 14-70 μm (under localized overloading, leading to damaged components) [60]–[62]. The average size of the wear particles

from MM bearings is much smaller than the MPE particles, ranging from 30 to 100 nm [55], [63].

The primary biological response to polyethylene and ceramic particles is an innate immune response, as seen in the classic "foreign body reaction", leading to the recruitment of a large number of osteoclasts (cells responsible for bone resorption), macrophages, dendritic cells and fibroblasts in periprosthetic tissues, with the presence of very few infiltrating lymphocytes [64]–[66]. The response is illustrated in Figure 3.4.

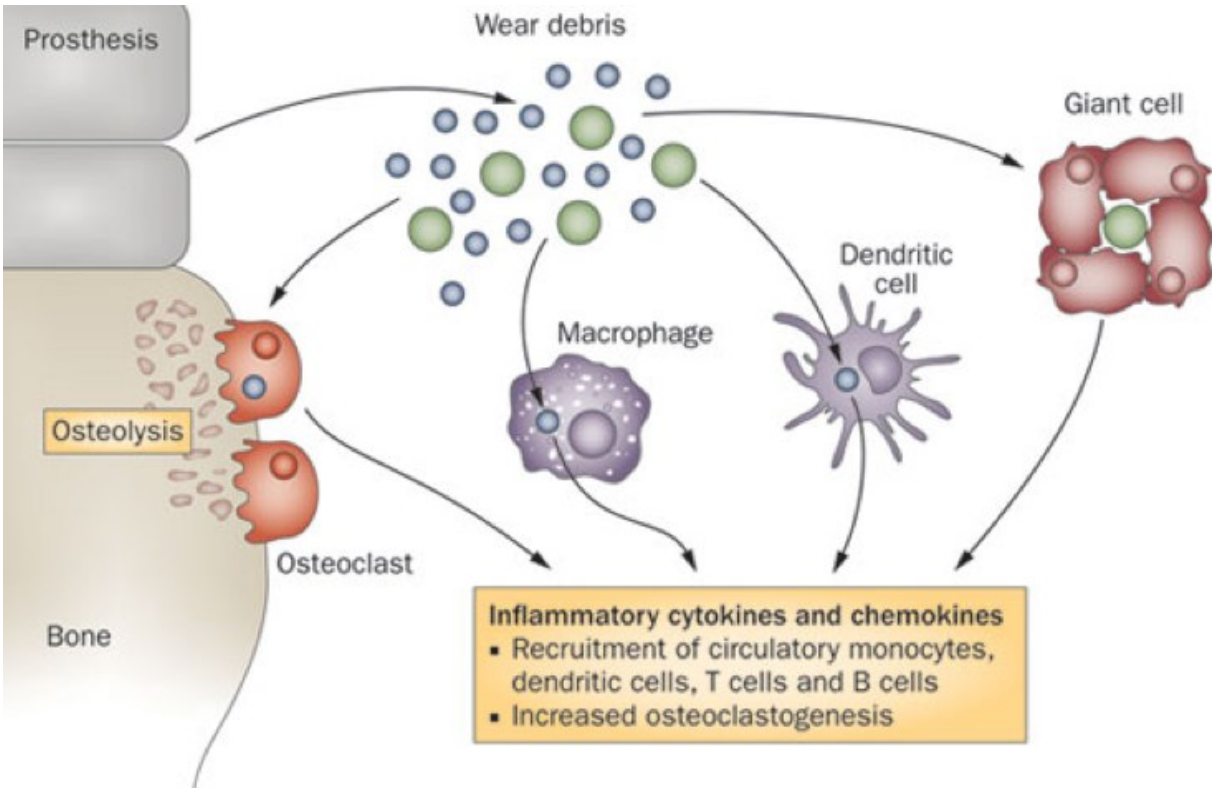

Figure 3.4 Biological cascades leading to periprosthetic osteolysis in response to wear particles in periprosthetic tissues. Reprinted by permission from Macmillan Publishers Ltd: Nature Reviews Rheumatology [49], copyright 2011.

Wear particles in the phagocytosable range (approximately 0.1 to 10 μm in diameter) undergo phagocytosis by osteoclasts, macrophages and dendritic cells, while larger particles and flakes (>20 μm) are phagocytozed by multinucleated giant cells formed by the fusion of macrophages [49]. The activation of osteoclasts, macrophages, dendritic cells and fibroblasts leads to the release of pro-inflammatory cytokines including interleukin (IL)-1, IL-6, tumor

necrosis factor-alpha (TNF-α), and receptor activator of nuclear factor κB ligand (RANKL), prostaglandin E2 (PGE2) as shown *in vitro* [67]–[70]. Similarly, histological analyses of periprosthetic tissues have shown of the presence of IL-1, IL-6 and TNF-α [71]–[73].

Some of the inflammatory cytokines and growth factors such as TNF-α, RANKL and macrophage colony-stimulating factor (M-CSF) play an important role in the differentiation of osteoclast progenitors into mature, multinucleated bone-resorbing osteoclasts at the bone-prosthesis interface [74]–[76]. Furthermore, several *in vitro* and *in vivo* studies have demonstrated that macrophages and recruited dendritic cells can also differentiate into multinucleated osteoclasts in the presence of M-CSF and RANKL [74], [77]–[79]. Therefore, the secreted inflammatory mediators can result in further exacerbation of osteoclastogenesis [49], leading to bone resorption.

Wear particles have also been shown to decrease bone formation by altering the function of the osteoblasts, cells responsible for forming new bone [80]. Indeed, several studies have shown that the released inflammatory cytokines and chemokines in response to wear particles inhibit the differentiation of the mesenchymal stem cells into mature osteoblasts [81], directly inhibit the collagen production by mature osteoblasts [82], and finally induce the apoptosis of these cells [83].

The biological effects of metal ions from implant wear and corrosion also remain a major cause for concern. Indeed, several studies have shown that metal ions can also induce the release of inflammatory mediators [12], [84]. In addition to this inflammatory response, metal ions may initiate a hypersensitivity reaction by forming organometallic complexes with serum proteins [43], [85], [86].

Taken together, the complex cellular response to implant wear particles and metal ions leads to the secretion of inflammatory and osteoclastogenic cytokines, which lead to the net bone loss surrounding the implant, thereby resulting in implant aseptic loosening [49]. Because wear particle-induced inflammatory response is by far the most common long-term post-surgery complication leading to revision surgery [4], large efforts have been made to better regulate the mechanisms involved in this overall reaction to increase implant longevity.

3.5 Anti-inflammatory Agents for the Treatment of Aseptic Loosening

The postoperative use of anti-inflammatory drugs may increase the longevity of the implants by decreasing the inflammatory response and inhibiting the intercellular mechanisms leading to the osteoclast-osteoblast imbalance [87]. However, currently, no drug has been specifically approved for the treatment of wear particle-induced aseptic loosening. Nevertheless, several anti-inflammatory agents have been suggested as potential drug candidates for the prevention and treatment of aseptic loosening by modulating the inflammatory response.

3.5.1 Anti-tumor necrosis factor alpha (TNF-α)

As mentioned in Section 3.4, pro-inflammatory mediators such as TNF-α have been shown to play a central role in initiating wear particle-induced periprosthetic osteolysis, and therefore, they have been considered as a leading target for modulation of wear particle-induced inflammatory response. The efficacy of several anti-TNF-α drugs such as etanercept and pentoxyfylline have been studied for the treatment of wear particle-induced periprosthetic osteolysis [88]–[92].

Etanercept is a U.S. Food and Drug Administration (FDA)-approved drug commonly used for the treatment of rheumatoid arthritis. It works as the decoy receptor of TNF-α, and therefore prevents TNF-α from promoting an inflammation response [88]. Etanercept was shown to inhibit cytokine production from macrophages exposed to titanium particles and reduce osteoclastogenesis in a bone wafer pit assay [89]. *In vivo* studies also demonstrated that etanercept reduced osteoclastogenesis and bone resorption in a murine model of titanium particle-stimulated osteolysis [89]. However, the osteogenic benefits of the drug have yet to be demonstrated in clinical studies. A study by Schwarz et al. [90] reported on the efficacy of etanercept on the progression of the osteolytic lesion size in 19 patients with previously diagnosed periprosthetic osteolysis. However, the volumetric three dimensional (3D)-computerized tomography analysis demonstrated that there was no statistically significant difference between the drug and the placebo-treated groups, which was later suggested to be due to the lack of sufficient power to detect any differences [1]. Finally, although the authors showed that etanercept was tolerable in the 19 patients with no serious adverse effects over a one-year period, the administration of etanercept has recently been associated with some serious incidents of infections and sepsis, including fatalities in predisposed children and adolescence patients, in

addition to reactivation of latent tuberculosis and hepatitis B infections [93], [94]. Therefore, these side effects represent major disadvantages for the use of etanercept for the treatment of implant aseptic loosening.

Another anti-TNF-α drug named pentoxifyline that may have a potential therapeutic role in the treatment of periprosthetic osteolysis has also been studied [91], [92]. Pentoxifyline is a potent inhibitor of TNF-α and has been shown to inhibit the secretion of TNF-α and initiate the production of anti-inflammatory cytokines by human monocytes exposed to titanium particles [91]. In a clinical study by Pollice et al. [92], it was also shown that the oral administration of pentoxifyline significantly reduced TNF-α secretion from peripheral blood monocytes of eight healthy volunteers. However, further investigations are needed to evaluate the effects of pentoxifyline in a larger sample size and to test its clinical efficacy in patients with periprosthetic osteolysis.

3.5.2 Anti-inflammatory cytokines (interleukin-4 and 10)

In contrast to TNF-α and other pro-inflammatory mediators, which propagate the inflammatory response, anti-inflammatory cytokines such as IL-4 and IL-10 possess inhibitory properties and may be involved in reducing the release of bone-resorbing factors at the bone-implant interface [95], [96]. *In vitro* studies have demonstrated that the expression of TNF-α and IL-6 was inhibited by IL-10 in polymethylmethacrylate-exposed human monocytes/macrophages [95] and by IL-4 in titanium particle-stimulated monocytes/macrophages [96]. The mechanisms by which IL-4 and IL-10 modulate the monocyte/macrophage response to wear particles are still not fully understood, but may include a change in macrophage phagocytosis ability, cytokine cascade, interaction between cells, or a combination of these factors [95]. While there is a lack of clinical studies with these immunoregulatory cytokines, future studies are needed to fully unfold the mechanisms by which IL-4 and IL-10 lead to a lower secretion of bone resorbing cytokines by monocytes/macrophages.

3.5.3 Cyclooxygenase inhibitors

As mentioned in Section 3.4, PGE2 is another well-known pro-inflammatory mediator involved in the implant aseptic loosening and is mainly produced by a group of compounds named cyclooxygenases (COX) [68]. COX-2 has been proposed to be the principal COX responsible for the production of PGE2 by fibroblasts in periprosthetic tissues [68]. Celecoxib, a

nonsteroidal anti-inflammatory drug and selective COX-2 inhibitor, has been clinically used to relieve symptoms of arthritis (e.g., osteoarthritis) [97]. Indeed, Zhang et al. [98] showed that celecoxib reduced inflammation, local PGE2 production, and titanium particle-induced osteolysis in mice calvaria. These findings were in agreement with the results of Im et al. [99], who also showed that celecoxib suppressed periprosthetic osteolysis in the femur of rabbits implanted with a porous coated metal bar, and exposed to UHMWPE particles. However, no human clinical studies appear to have been conducted with celecoxib in patients with wear particle-induced periprosthetic osteolysis.

3.5.4 Statins, and more specifically simvastatin

The majority of the anti-inflammatory agents listed above have been shown to successfully inhibit periprosthetic osteolysis in animal models. However, very few have progressed to human clinical studies, and therefore there is a lack of clinical evidence for their efficacy in patients with wear particle-induced periprosthetic osteolysis. Furthermore, many of the anti-inflammatory agents are immunosuppressive and have serious side effects (e.g., strong anti-anabolic effects) [100]. Therefore, given the multiple targets of the biological pathways involved in aseptic loosening, it is fundamental to find a pleiotropic drug with tolerable side effects.

Statins are amongst the most commonly prescribed medications worldwide, used as cholesterol lowering agents for the prevention and treatment of cardiovascular and coronary heart disorders [101]. At low doses (20 mg/day), statin monotherapy has been shown to be clinically safe with tolerable side effects [102]. Statins target the liver to inhibit the production of cholesterol mainly because the liver produces the most circulating cholesterol in the blood when compared to the diet. In order to reduce the cholesterol synthesis in the liver, statins act by competitively inhibiting an enzyme named 3-hydroxy-3-methylglutaryl coenzyme A (HMG-CoA) reductase, the first and main rate-limiting enzyme involved in the cholesterol synthesis pathway. This competition results in the reduced production of mevalonate, which is not only the precursor for cholesterol synthesis, but also for many other non-steroidal isoprenoidic molecules [103].

The inhibition of the HMG-CoA enzyme followed by the blockage of the mevalonate pathway by statins are reported to lead to several effects (independent of the

hypocholesterolemic effects) [104], which could contribute to the treatment of implant wear-mediated periprosthetic osteolysis. Interestingly, two recent clinical studies have shown that patients using statins had substantially reduced risks of developing femoral osteolysis [105] and undergoing revision surgery following a primary THR [106].

Simvastatin, a synthetic FDA-approved statin, is commonly prescribed for the treatment of hypercholesterolemia and is administered orally in the form of tablets [107]. The pro-drug consists of a 6-membered lactone ring (Figure 3.5), which is enzymatically and chemically hydrolyzed *in vivo* in the liver, intestines, and blood plasma to form the pharmacologically active metabolite, beta-delta-dihydroxy acid [108].

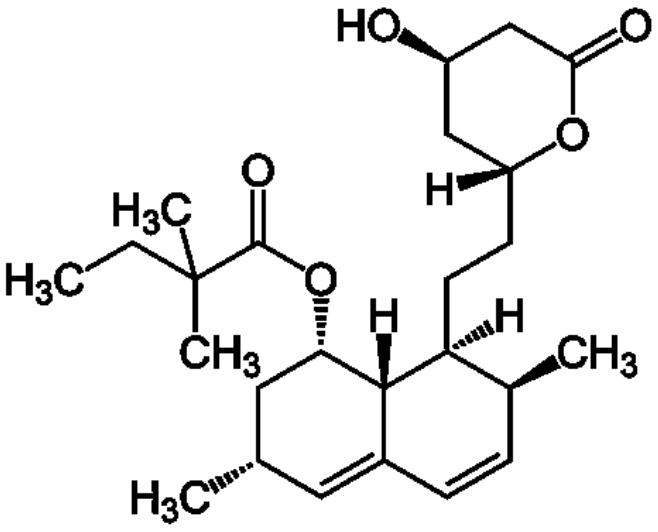

Figure 3.5 Molecular structure of simvastatin [109].

The activated simvastatin is structurally similar to HMG-CoA (substrate of HMG-CoA reductase), which, as previously mentioned, inhibits the synthesis of cholesterol and prenylated proteins [103], leading to several therapeutic effects that could potentially benefit patients with implant wear-mediated periprosthetic osteolysis. Simvastatin has been shown to possess anti-inflammatory and immunoregulatory properties both *in vitro* and *in vivo*, depicted by the reduced production of inflammatory markers such a C-Reactive Protein in blood plasma [9], [110]. Simvastatin was also shown to enhance the phagocytic capacity of macrophages by improving the cell membrane fluidity as a result of the decreased cholesterol content of the cell membrane [111]. Even though it is challenging to differentiate the proposed direct anti-inflammatory action from the effects based on cholesterol-lowering property in human clinical studies [9], evidence

from several animal model studies has well supported the anti-inflammatory activity of statins from their lipid-lowering action [112]–[114]. Another interesting effect of simvastatin is its ability to increase the expression of several bone growth regulatory factors such as bone morphogenetic protein-2, vascular endothelial growth factor, type I collagen, osteocalcin and bone sialoprotein [115], [116]. These studies suggest the beneficial effects of simvastatin on osteoporosis and bone fractures by stimulating bone regeneration [117].

An additional property of simvastatin that is beneficial for counteracting the adverse responses shown in wear-mediated osteolysis is its inhibitory effects on osteoclast activity and the subsequent osteoclast-mediated bone loss [10], [11]. Indeed, it is suggested that simvastatin decreases osteoclastogenesis by reducing the synthesis of prenylated protein (in particular GTPases), which are shown to be crucial for the function of osteoclasts [11].

Therefore, the pleiotropic properties of simvastatin including inhibition of inflammatory response, increased bone regeneration, and decreased bone loss make this drug a promising therapeutic agent for the treatment of implant aseptic loosening.

3.6 Local and Controlled Delivery of Simvastatin

As discussed in Section 3.5, the oral administration of several anti-inflammatory drugs has been proposed for the modulation of the inflammatory response in patients with periprosthetic osteolysis. However, up to date, there is no approved drug for the treatment and prevention of periprosthetic inflammation, mainly due to the lack of an efficient and tissue-specific drug delivery system [1]. Indeed, the use of a systemic drug administration poses several limitations including a lack of tissue specificity and therefore efficacy, a need for a higher dose due to the first-pass metabolism of the liver, and systemic side effects [118].

The oral administration of simvastatin may result in the delivery of insufficient drug dosages to the periprosthetic tissues that may not have any significant therapeutic effects, as shown in a 1-year clinical study on osteoporosis with a daily oral administration of 40 mg simvastatin [119]. In addition, high doses of simvastatin (40-80 mg/day) have been associated with higher risks for developing adverse side effects such as rhabdomyolysis [120], liver failure [121], and acute kidney injury [122]. To prevent these side effects, several studies using animal models were performed using local injections of simvastatin (without the use of a delivery

system) to improve bone growth [123], [124] and to strengthen bone structure [125]. However, the local administration of statins without a delivery system to control the release has been shown to result in soft-tissue inflammation [126]–[128]. Furthermore, other limitations with local injections of simvastatin include short-term therapeutic effect, increased health care costs, and poor patient's compliance due to the frequent drug injections [129]. On the other hand, the use of a drug delivery system that allows the controlled release of the drug not only overcomes the aforementioned limitations, but can also provide predictability in drug release kinetics [129]. Therefore, to use simvastatin in the context of modulating periprosthetic osteolysis, it is fundamental to develop an appropriate drug delivery system that would allow the local and sustained release of simvastatin in periprosthetic tissues.

To date, research on the development of a simvastatin delivery system has been limited. Some efforts have been made to develop an efficient drug delivery system to evaluate the bone growth-stimulating properties of simvastatin [14], [130]. For example, Chou et al. [14] used a marine exoskeleton made of fossilized coral-derived beta-tricalcium phosphate (β-TCP) as a drug delivery scaffold to evaluate the *in vitro* release of simvastatin from non-coated and apatite-coated scaffolds. The release kinetic studies showed that non-coated β-TCP released 48% of simvastatin in simulated body fluid (SBF) over the course of seven days, whereas apatite-coated β-TCP significantly delayed the release by 20%. The apatite coating of the scaffold appeared to be promising in slowing the release of simvastatin, but data on longer-term release (after seven days) are lacking. The administration route proposed by the authors for this drug delivery system was through implantation in the site of trauma (bone-related fractures) or in the muscles adjacent to the affected bone, with the overall aim of stimulating bone growth. However, future studies are needed to evaluate the efficacy of this drug delivery system in cell cultures and *in vivo*.

Another study by Tai et al. [130] developed a drug delivery system composed of poly(lactic-co-glycolic acid)/hydroxyapatite (PLGA/HAp) microspheres delivered locally to evaluate the bone repair properties of pre-activated simvastatin in a mouse model. The microspheres were synthesized using the water-in-oil-in-water (w/o/w) double emulsion technique, with a reported simvastatin encapsulation efficiency of 77.7±10.3%. The release kinetic studies showed a burst release of 0.53-0.24 μg of simvastatin (representing approximately 40% of the encapsulated drug) within two days, and over half of the encapsulated amount after 14 days. However, at the end of the release kinetic, the remaining mass of simvastatin inside the

PLGA/HAp microspheres (non-released simvastatin) was not determined. Therefore, it is not clear if this mass would add up with the mass of released simvastatin to equate the reported encapsulated mass. Overall, results showed that the slow release of simvastatin enhanced initial callus formation, cell growth in the grafted bone, thereby improving bone healing quality.

The encapsulation of simvastatin in PLGA-based delivery system is promising due to the hydrophobic nature of both simvastatin and PLGA. However, despite the advantages of PLGA, which also include its biocompatibility, the preparation of drug delivery systems (in the form of microspheres, nanoparticles, hydrogel films, etc.) with synthetic polymers such as PLGA is complex and requires organic solvents that can adversely affect the drug stability [131]. PLGA hydrogels also degrade at a relatively fast rate in the human body [132], which may be a limiting factor for long-term delivery of pharmaceutical agents. In contrast, water-soluble polymers such as alginate (as will be discussed in Section 3.8) offer mild and simple preparation methods without the use of noxious organic solvents, thereby minimizing the toxicological and environmental problems associated with solvents [133]. However, the poor solubility of simvastatin in hydrophilic polymers remains the main challenge for the development of an efficient drug delivery system.

3.7 Increased Solubility of Simvastatin with 2-Hydroxypropyl-β-Cyclodextrin

Simvastatin is categorized as a class II drug (lipophilic) in the Biopharmaceutics Classification System, due to its low aqueous solubility (0.76 mg/L) and low oral bioavailability (5%) [134]. Therefore, to use simvastatin in a hydrophilic matrix, its solubility as well as stability need to be increased.

Cyclodextrins are cyclic oligosaccharides, which are formed during bacterial digestion of starch and are known to be useful pharmaceutical excipients [135]. These molecules form a unique truncated cone-shaped structure, with a hydrophilic outer shell and a relatively hydrophobic inner core, with the latter allowing the formation of non-covalent hydrophobic interaction with hydrophobic organic compounds [136]. As a result, cyclodextrins can form water-soluble inclusion complexes, thereby improving the aqueous solubility and bioavailability of hydrophobic compounds. The most commonly used cyclodextrins include α-, β- and γ-cyclodextrin, which are composed of 6, 7, and 8 number of α-1-4-linked glucose units in the hydrophobic ring, respectively. Since the number of glucose units determines the size of the

inner ring, different types of cyclodextrins have been used for the complexation of pharmaceutical agents with different sizes [136].

2-hydroxylpropyl-β-cyclodextrin (HP-βCD), a hydroxyalkyl derivative of βCD, has been reported to possess improved water solubility compared to βCD [136], due to the presence of hydroxylpropyl groups on the shell, as depicted in Figure 3.6.

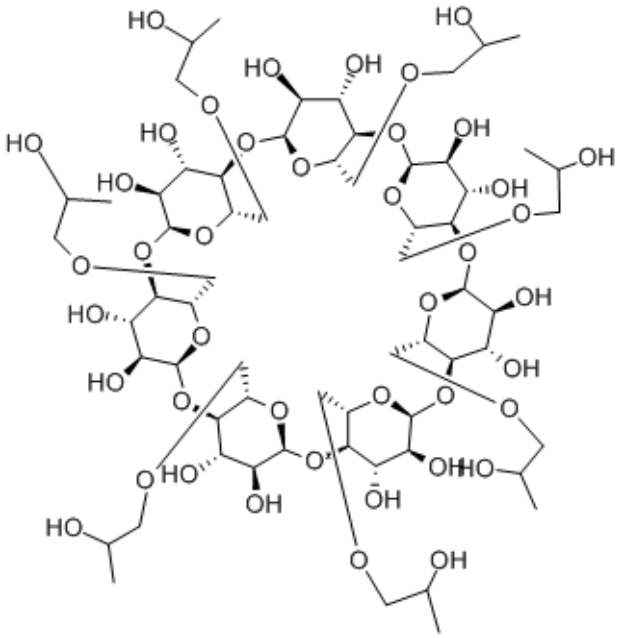

Figure 3.6 The molecular structure of 2-hydroxypropyl-β-cyclodextrin (HP-βCD) [137].

HP-βCD is FDA-approved [138], and toxicological studies in animals and humans have shown that it is well tolerated [136]. Simvastatin molecules, activated or not, are reported to form a 1:1 stoichiometric inclusion complexes with HP-βCD [139]. Indeed, Ungaro et al. [108] showed by ultra violet-assisted reverse phase high performance liquid chromatography analysis that the inactivated simvastatin molecules (i.e., with a closed lactone ring) could still undergo hydrolysis of the lactone ring (i.e., opening of the lactone ring) when complexed with HP-βCD, suggesting that the interaction of simvastatin with HP-βCD did not involve the lactone ring of the molecule. The authors further demonstrated by nuclear magnetic resonance that the lactone ring of simvastatin was not included inside the hydrophobic core of HP-βCD. Overall, their results suggested that the inactivated and activated simvastatin molecules interacted with HP-βCD in a similar way.

The majority of studies have prepared inclusion complexes of simvastatin with HP-βCD or βCD using various techniques such as the supercritical antisolvent process [139], simple physical mixing, kneading, spray drying [140], and co-precipitation method [141], with the aim of increasing simvastatin bioavailability and dissolution rate for oral drug administration. For instance, Jun et al. [139] demonstrated that the oral administration of simvastatin (not pre-activated) complexed with HP-βCD in rats resulted in significantly reduced total cholesterol and triglyceride serum levels in comparison to the non-complexed simvastatin. Nevertheless, while the results of these studies are very promising in terms of improved bioavailability of complexed simvastatin, very few studies have focused on developing complexation techniques to increase the solubility of pre-activated simvastatin for local drug delivery applications.

Yoshinari et al. [142] developed a complexation technique for pre-activated simvastatin and β-CD to be used for local and controlled release of simvastatin from films coated onto titanium substrates. In this process, the pH of the activated simvastatin solution was decreased to 4.2 (slightly higher than the pK_a of the carboxylic group of the opened lactone ring), prior to the physical mixing of simvastatin with βCD at the molar ratio of 1:2. The decrease in pH was performed in order to further increase the hydrophobic affinity of simvastatin, thereby improving the complexation process. The ultra violet spectroscopy analysis of the dissolved simvastatin showed that at pH 4.2, simvastatin was complexed with βCD at 79% and was released more slowly from coatings of titanium plates than at higher pH [142]. This technique appeared promising for increasing the solubility of simvastatin in aqueous solution for local drug delivery applications, and may be further improved by using HP-βCD instead of βCD, as well as higher molar ratio of HP-βCD to simvastatin.

3.8 Alginate Polymer for Drug Delivery

3.8.1 Structure of alginate

Sodium alginate is an aqueous soluble salt of alginic acid, which has attracted much interest for drug delivery applications because of its biocompatibility, low toxicity, relatively low cost, and mild gelation conditions [15], [16]. Alginate is a naturally occurring anionic polysaccharide, derived from marine brown algae and some species of bacteria. It is composed of β-D-mannuronic acid (M) and α-L-guluronic acid (G) residues, linked together by 1,4-glycosidic bonds [133]. As shown in Figure 3.7, the M-block regions are flat and ribbon-like due to the

equatorial binding, while the G-block regions are buckled with a pleated conformation because of the axial glycosidic linkage [133]. The composition and sequence of the M and G residues as well as the chain molecular weight differ in various available types of alginate, and depend primarily on the source of the brown algae (e.g., the species, section, age, season of harvest, etc.) from which the alginate is obtained [17], [133]. For instance, alginate isolated from the stem of old *Laminaria hyperborea* brown algae possesses a large amount of G residues, while alginate from *Ascophyllum nodosum* and *Laminaria japonica* contains a low amount of G residues [133].

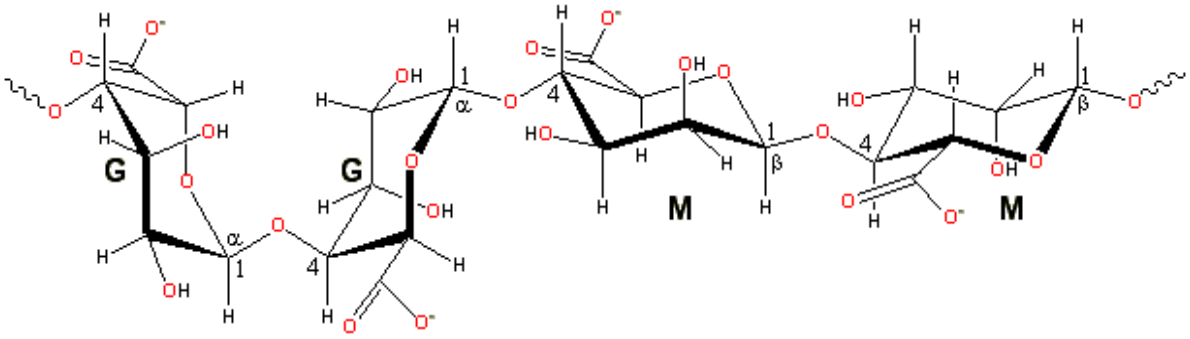

Figure 3.7 Molecular structure of alginate for a GGMM block region [143].

The alginate hydrogel with a large amount of G residues is stronger, stiffer and has a smaller pore size. It allows limited movement of the solutes from and into the cross-linked hydrogel, which is advantageous for the encapsulation of small molecules [133]. On the other hand, a larger amount of M residues leads to the formation of a more elastic and weaker alginate hydrogel [15]. Nevertheless, the physiochemical properties of alginate can be easily altered via chemical and physical reactions in order to accommodate a wide range of drug delivery applications [144].

3.8.2 External gelation technique for the preparation of alginate hydrogel

The most commonly used method to form a 3D alginate hydrogel is the external ionic gelation technique, in which the aqueous sodium alginate mixed with the molecules to be encapsulated is extruded drop-wise into a gelation medium containing di- or poly-valent ions such as Ca^{2+} [145]. In this case, the sodium ions of the G residues are substituted by Ca^{2+}, resulting in the formation of a so-called egg-box gel structure that encompasses tightly held ionic bridges between the G blocks of the two adjacent polymer chains [146], as depicted in Figure 3.8.

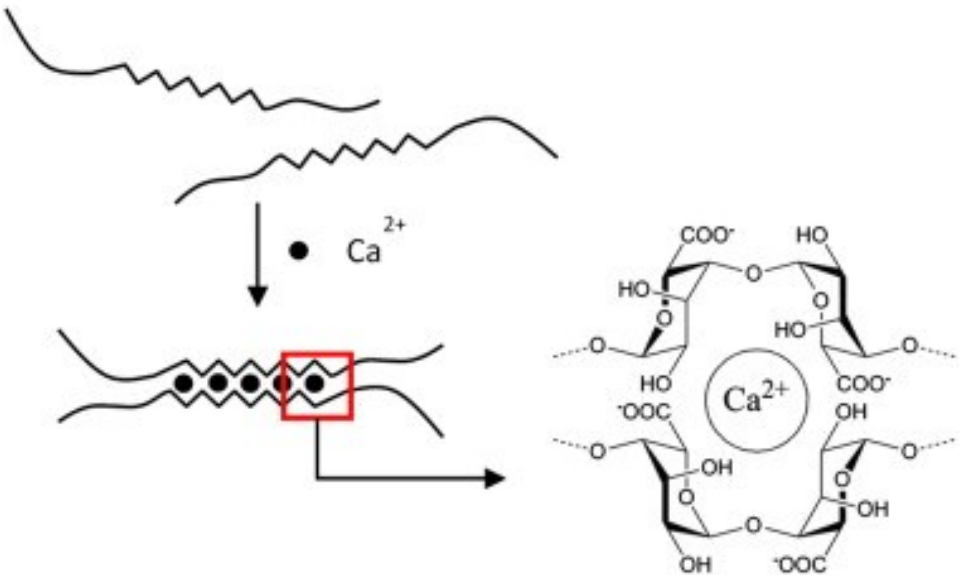

Figure 3.8 Cross-linking of alginate molecules with Ca^{2+} ions. Reprinted from [144] with permission from Elsevier.

Therefore, the instantaneous cross-linking of the alginate chains by Ca^{2+} results in the encapsulation of the desired material in a 3D lattice [133]. This cross-linking behaviour occurs under mild gelation conditions and using non-toxic chemicals, which is desirable for the encapsulation of cells, proteins and other sensitive biomolecules in order to retain their full biological activity [17]. The high Ca^{2+} content of alginate hydrogel has been shown to possess stimulatory properties for osteoblast proliferation [147], which is also a valuable advantage of alginate as a drug delivery system in the context of modulating wear-mediated periprosthetic osteolysis. Finally, the degradation rate of the ionically cross-linked alginate hydrogel is remarkably slow (up to months or years), and mainly depends on the dissolution of the cross-linking ions (e.g., Ca^{2+}) since the alginate hydrogel is not naturally degraded in mammals via enzymatic reactions [18]–[20], [148]. This property of alginate may be favourable for the local and prolonged release of simvastatin.

3.8.3 Alginate nano- vs. microspheres

Biodegradable alginate nano- and microspheres are commonly used for drug delivery applications because they are easy to administer and they do not need to be surgically removed [133]. They can be used to encapsulate many different types of pharmaceutical agents, which

they protect from the harsh environment inside the body [149]. Their size (nano- or microscale) depends on their application.

Polymeric nanospheres (also called nanoparticles) are commonly used as short-term drug delivery vehicles, and are administered via various routes such as oral, intravenous, subcutaneous, intramuscular or transdermal [150]. For instance, alginate-based nanospheres are commonly used orally as a drug delivery system for gastrointestinal (GI) applications since they can be easily uptaken by the cells of the GI track because of their smaller size [21], [131]. Similarly, alginate-based nanospheres have attracted interest in drug delivery research for cancer applications [151]–[154] due to their ability to pass through the pores of the leaky blood vessels surrounding the targeted tumours [155].

On the other hand, polymeric microspheres are mainly used as long-acting drug carriers, and are reported to remain in the injection site due to their larger size (especially for spheres larger than 5 μm in diameter) [150]. In addition, they can encapsulate more drugs in comparison to nanospheres [150]. More specifically, alginate-based microspheres have been extensively used for the encapsulation of a wide range of bioactive molecules, including DNA [156], [157], proteins [147], [158]–[164] enzymes [165]–[167], and antibodies [168], [169], as well as cells [147], [170]–[175]. They have been used for various medical applications including but not limited to GI [156], [158], [161], [164], as well as in cell culture and tissue engineering studies [146], [173], [174]. Therefore, alginate microspheres appear to be most suitable for prolonged and local release of simvastatin in periprosthetic tissues.

3.8.4 Encapsulation efficiency in alginate microspheres

The first step for the development of a drug delivery system is to optimize the encapsulation efficiency. Numerous studies have used alginate microspheres/beads for the encapsulation of a wide range of pharmaceutical agents and bioactive components [147], [156]–[169]. Interestingly, with the use of the external gelation technique for the microsphere synthesis, several studies report an indirect method for measuring the encapsulation efficiency [23], [130], [164], [169], [176], in which the mass of the non-encapsulated drug in the gelation medium is subtracted from the initial mass of the drug in order to determine the mass of encapsulated drug. While this method is easy, it may lead to an overestimation of the encapsulation efficiency since it only accounts for the loss of the pharmaceutical agents in the final stage of the encapsulation

process [177], and does not account for the mass of the drug left in the experimental apparatus (e.g., syringes, containers, etc.) or degraded during the synthesis process prior to the microsphere formation in the gelation medium. This may be the reason why only a partial release of encapsulated pharmaceutical agents is reported at the end of many release kinetic studies [23], [167], [178]. Therefore, a more reliable method to measure the encapsulation efficiency is via direct measurement, in which the microspheres are dissolved in order to directly determine the mass of the encapsulated drug [179]–[181].

3.8.5 Limitations of alginate microspheres

High encapsulation efficiencies have been commonly reported with macromolecules such as proteins, growth factors, vaccines, probiotics, and cells in alginate microspheres, ranging from 80 to 95% [159], [179], [182], [183]. The nanoporous matrix of alginate microspheres, which typically ranges from 5 to 200 nm [184], allows the exchange of nutrients, gases and waste materials and may therefore be advantageous for the encapsulation of cells by prolonging their viability [185]. However, the large porosity poses challenges for the encapsulation of small drugs since it facilitates their rapid diffusion during the microsphere synthesis process [15], [23].

Low encapsulation efficiencies have been reported with low molecular weight pharmaceutical agents, including 4% for nitrofurantoin in 2.0% (w/v) alginate microcapsules [168]. Other studies have reported higher encapsulation efficiencies, up to 32% for indomethacin in 4.0% (w/v) alginate beads [186], and 43% for propranolol-HCl in 3.0% (w/v) alginate beads [23], likely because of differences in the measurement methods (direct vs. indirect, as previously explained in Section 3.8.4). Another low molecular weight drug named furbiprofen was encapsulated in periodate-oxidized alginate beads (2.5% (w/v) alginate) with an encapsulation efficiency of 89% [22]. Despite the small size of flurbiprofen, the high encapsulation efficiency may be explained by the chemical modifications of alginate, including the covalent cross-linking of the alginate beads with adipic dihydrazide (ADH) in addition to Ca^{2+} ions. The ADH-treated alginate beads sustained the release of the encapsulated furbiprofen for 8 hours at physiological pH. However, the untreated beads released all the encapsulated drug within merely 1.5 hours, which was primarily attributed to its rapid diffusion. Therefore, the large porosity of microspheres has been a limiting factor for the use of alginate microspheres for prolonged release of low molecular weight drugs [15].

As a result, to overcome the aforementioned disadvantage of the alginate microspheres, several approaches have been adopted by researchers to reduce the diffusion rate of low molecular weight drugs, and thereby improving the encapsulation efficiency, as explained in next section.

3.8.6 Strategies for improving the drug encapsulation efficiency in alginate microspheres

In order to improve the encapsulation efficiency of pharmaceutical agents, sodium alginate solution has been used in combination with different polymers such as pectin [187] [188], methylcellulose [189], chitosan [161], [190], and dextran sulfate [23], [164].

Chitosan is the N-deacetylated derivative of chitin, which is isolated from various species of marine crustaceans and insects [191]. Chitosan is a biocompatible, non-immunogenic, non-toxic, biodegradable and inexpensive cationic polysaccharide, which has been extensively used in combination with alginate microspheres as a coating agent for drug delivery applications [192]–[194]. The positively-charged amino groups of chitosan form ionic bonds with the negatively-charged carboxyl groups of alginate, resulting in the formation of strong electrostatic complexes in the outer layer of alginate microspheres, thereby reducing the pore size of this layer. The chitosan layer also decreases the dissolution rate of alginate chains by restricting the influx of water and calcium chelator agents into the calcium alginate matrix [195]. It is therefore advantageous for stabilizing the alginate gel, and consequently shielding the microspheres from leaching the low molecular weight drug during the microsphere synthesis process [133], [149], [196].

Dextran sulfate is a high molecular weight, branched-chain derivative of the polysaccharide dextran obtained from esterification of dextran molecules with chlorosulphonic acid [197]. It is a biocompatible and biodegradable polyanion, which can form strong electrostatic interactions with polycationic polymers, such as chitosan [147]. Due to the anionic nature of both dextran sulfate and alginate, the ionically cross-linked blended polymer forms a denser gel network with the chitosan coating compared to alginate alone, leading to a reduced pore size of the chitosan coating layer, thereby decreasing the permeability of the microspheres [23]. A denser polymer network may decrease the diffusion of low molecular weight drugs out of the microsphere matrix and into the gelation medium during the microsphere synthesis process, leading to higher encapsulation efficiency [23], [164].

Interestingly, a recent study by Khorram et al. [23] showed that dextran sulfate-reinforced alginate microspheres coated with chitosan led to the highest encapsulation efficiency of a low molecular weight drug (propranolol-HCl), when compared to alginate microspheres, and chitosan-coated alginate microspheres. More specifically, the coating of the 3.0% (w/v) alginate microspheres with chitosan significantly improved the encapsulation efficiency from 43.1% to 53.8%, which was further increased to 70.8% when reinforcing the chitosan-coated alginate microspheres with 1.0% (w/v) dextran sulfate. Despite the indirect encapsulation efficiency measurements, which may have resulted in an overestimation of the encapsulation efficiency, the chitosan coating of the alginate microspheres and the addition of dextran sulfate to the alginate solution appeared promising to improve the encapsulation efficiency of low molecular weight drugs.

4 Manuscript

4.1 Foreword

As described in great detail in the literature review, there is currently a clinical need to modulate periprosthetic osteolysis in order to improve implant longevity. The focus of this thesis was on the initial steps of the development of a drug delivery system made of alginate-based microspheres for simvastatin release, with the long-term goal of providing a local delivery of simvastatin in the periprosthetic tissues to modulate the surrounding inflammatory response leading to periprosthetic osteolysis. The results of this study are included in a manuscript being finalized to be submitted to the Journal of Biomedical Materials Research Part B: Applied Biomaterials, and entitled: "Simvastatin encapsulation in alginate-based microspheres". All data presented in the manuscript were obtained and analyzed by myself. The manuscript was written by myself and reviewed by Dr. Isabelle Catelas. Additional experimental details are provided in:

- Appendix A: Pre-extrusion steps for microsphere synthesis;
- Appendix B: Illustration of the experimental set-up for the extrusion process;
- Appendix C: Example of calculation tables for simvastatin preparation and complexation with HP-βCD; and
- Appendix D: Example of a standard curve used to measure the concentration of simvastatin complexed with HP-βCD.

4.2 Abstract

Simvastatin appears to be a promising drug for the modulation of the inflammatory response to joint implant wear particles and metal ions due to its anti-inflammatory properties, as well as its ability to stimulate bone formation and decrease bone loss. Alginate has been extensively used in various drug delivery applications due to its biocompatibility, non-immunogenicity, and biodegradability. However, drawbacks include the difficulty to encapsulate hydrophobic drugs, and the large pore size of alginate microspheres leading to drug leakage. Therefore, the objective of this study was to increase simvastatin encapsulation in alginate-based microspheres by: 1. Complexing simvastatin with 2-hydroxypropyl-β-cyclodextrin (HP-βCD) to increase its solubility; and 2. Coating the alginate microspheres with chitosan, adding dextran sulfate in the alginate solution, and optimizing the gelation conditions. The highest complexation

of simvastatin with HP-βCD (97.6%) was obtained when using the highest HP-βCD to simvastatin molar ratio (10). Chitosan coating of the alginate microspheres increased simvastatin encapsulation efficiency up to 10.6%, which was further increased to 14.0% when adding 2.0% (w/v) dextran sulfate in the alginate solution, and to 22.4% when supplementing the gelation medium with 0.263 mM simvastatin. These approaches increased simvastatin encapsulation efficiency. However, future studies should investigate additional diffusion barriers to further increase the encapsulation efficiency.

4.3 Introduction

Despite the great success of the total joint replacement surgeries, there are still several mechanisms of failure, including aseptic loosening due to periprosthetic osteolysis that limit the implant longevity [4]. Specifically, wear particles from the implant have been shown to greatly contribute to periprosthetic osteolysis by inducing an inflammatory response [6]. The postoperative use of anti-inflammatory drugs has been shown to regulate the inflammatory response, leading to an increased implant longevity [87]. Simvastatin, an FDA-approved cholesterol-lowering statin, has been shown to possess anti-inflammatory properties [12], to stimulate bone growth [8], [127], and to inhibit bone loss [10], [11], all counteracting the mechanisms involved in implant aseptic loosening. As a result, simvastatin appears to be a promising drug to increase implant longevity, and thereby delaying the need of a revision surgery. However, some studies have shown that the local injection of statins in the absence of a drug delivery system to control the release can lead to an inflammatory response [126], [127]. There is therefore a clinical need for the development of a drug delivery system that would allow the controlled and local release of simvastatin.

Previous drug delivery systems used for simvastatin include poly(lactic-co-glycolic acid)/hydroxyapatite microspheres [130] and fossilized coral-derived beta-tricalcium phosphate scaffold [14]. However, the drug release from these delivery systems was primarily limited by the rapid degradation/dissolution of the polymer/scaffold used. Therefore, it is critical to develop a drug delivery system made of a longer lasting biodegradable and biocompatible material, with the goal of providing a longer and sustained drug release.

Sodium alginate, an aqueous soluble salt of alginic acid, is a naturally occurring polysaccharide of (1–4)-linked β-D-mannuronic acid and α-L-guluronic acid that has attracted

much interest in drug delivery applications because of its biocompatibility, low toxicity, relatively low cost, and mild gelation conditions [15], [16]. The degradation rate of the ionically cross-linked alginate hydrogel is remarkably slow (up to months or years), mainly relying on the dissolution of the cross-linking ions (e.g., Ca^{2+}) in the surrounding medium since the alginate hydrogel is not naturally degraded in mammals via enzymatic reactions [18]–[20]. This property of alginate may therefore be favourable for the local and prolonged release of simvastatin.

Numerous studies have used alginate microspheres for the encapsulation of large bio-macromolecules such as proteins [147], [158]–[164], [179] and cells [147], [170]–[175]. However, the encapsulation of simvastatin in alginate microspheres is more challenging because of its hydrophobicity and low molecular weight. Indeed, the pore size of alginate microspheres has been shown to range between 5 and 200 nm depending on the concentration of alginate [184], which can cause the drug leakage during the microsphere synthesis. Previous studies have shown that the use of 2-hydroxypropyl-β-cyclodextrin (HP-βCD) improves the solubility and stability of simvastatin in aqueous solutions [139], [140], [176]. HP-βCD is a highly water-soluble cyclic oligosaccharide, composed of a hydrophilic outer layer and a hydrophobic cavity, wherein the latter allows the formation of non-covalent bonds with simvastatin [176]. Therefore, the complexation of HP-βCD with simvastatin may allow increasing simvastatin solubility in alginate microspheres.

In order to improve the encapsulation of pharmaceutical agents, alginate has been commonly used in combination with other polymers including chitosan [159], [161], [163], [170], [171], [192], [194], [198], [199], and dextran sulfate [23], [164]. Chitosan is a naturally-derived cationic polysaccharide that forms strong electrostatic bonds with alginate molecules, thereby forming a denser outer layer [199]. It has therefore been used as a coating polymer for alginate microspheres in drug delivery applications [192], [198], [199]. Interestingly, chitosan has also been shown to increase the mechanical strength of alginate microspheres [192], [200]. On the other hand, dextran sulfate, a branched-chain anionic polymer of sulfated glucose, was reported to possibly increase the density of the alginate, and thereby reduce the pore size and permeability of alginate microspheres [23], [164]. The combination of chitosan and dextran sulfate with alginate may therefore allow maximizing the encapsulation of simvastatin in alginate-based microspheres.

The objective of this study was to increase simvastatin encapsulation in alginate microspheres by complexing simvastatin with HP-βCD to increase its solubility and by coating the alginate microspheres with chitosan, adding dextran sulfate in the alginate solution, and optimizing the gelation conditions. The resulting microspheres were then characterized in terms of size and morphology.

4.4 Materials and Methods

4.4.1 Preparation and activation of simvastatin

Simvastatin (Catalogue No. 10010345; Cayman Chemical, Ann Arbor, MI) was activated as recommended by the supplier, following the protocol of Sadeghi et al. [201]. Briefly, 4 mg of simvastatin were dissolved in 100 µL of absolute ethanol (Commercial Alcohols Inc, Toronto, ON) in siliconized eppendorf tubes (Fisher Scientific International Inc., Hampton, NH), and the solution was alkanized with 150 µL of 0.1 N sodium hydroxide. The solution was then mixed thoroughly, followed by a 2h incubation at 50° C to activate simvastatin (i.e., convert the drug into its pharmacologically active free-acid form). After the incubation, the solution was thermally equilibrated to room temperature and the pH was adjusted to 4.2 with 0.5 N hydrogen chloride in order to protonate the carboxyl group of the lactone ring. This has been suggested to increase the hydrophobicity of simvastatin, leading to a more effective complexation process with βCD [142].

4.4.2 Simvastatin complexation with HP-βCD

HP-βCD (Acros Organics, Geel, Belgium) was used as a drug excipient in order to increase the solubility of simvastatin in alginate solution. The procedure of simvastatin complexation with HP-βCD was adopted from Yoshinari et al. [142], with some adjustments. Briefly, HP-βCD powder was added to a 35 mM activated simvastatin solution at a molar ratio of 2, 4, 6, 8, or 10. The solutions were then stirred at 700 rpm and 50° C for 15 minutes in a water-filled beaker placed on a heating stir plate. After the incubation, the solutions were thermally equilibrated to room temperature and centrifuged at 6,000 g and 4° C for 15 minutes in order to precipitate the undissolved simvastatin. Simvastatin absorbance of the supernatants was then measured at 238 nm using a hybrid microplate reader (Synergy™ 4; BioTek, Winooski, VT) to determine simvastatin mass in the solutions. Standard curves were prepared using non-

complexed simvastatin in double-distilled water (simvastatin absorbance is not affected by its complexation with HP-βCD, and therefore non-complexed simvastatin can be used for the standard curves). The percentage of simvastatin complexation with HP-βCD (%) was then calculated as the ratio of simvastatin mass in the supernatant to the simvastatin mass initially used.

4.4.3 Preparation of gelation medium and alginate solution with or without dextran sulfate

The gelation medium used for the extrusion consisted of $CaCl_2$ solution with or without the addition of medium molecular weight chitosan to analyze the effects of chitosan coating on simvastatin encapsulation efficiency in the alginate microspheres. For the synthesis of microspheres without chitosan, $CaCl_2$ solution was prepared by dissolving dehydrated $CaCl_2$ powder (EMD Chemicals Inc, Gibbstown, NJ) in distilled water to a final concentration of 5.0% (w/v), under stirring conditions at room temperature. For the synthesis of chitosan-coated microspheres, 0.1% (w/v) chitosan solution was first prepared by dissolving medium molecular weight chitosan powder (viscosity of 50-100 mPa.s; TCI, Tokyo, Japan) in 1.0% (v/v) glacial acetic acid (Fisher Chemicals, Pittsburgh, PA) under stirring conditions at room temperature until the chitosan was completely dissolved. Dehydrated $CaCl_2$ powder was then added to the chitosan solution to a final concentration of 5.0% (w/v). The resulting 5.0% (w/v) $CaCl_2$ – 0.1% (w/v) chitosan solution was then mixed under stirring conditions at room temperature until the $CaCl_2$ powder was completely dissolved, followed by filtration using a 0.45 μm membrane filter (Pall Corporation, Ann Arbor, MI) to remove any undissolved chitosan residues.

Alginate solution was prepared by dissolving alginate powder (low viscosity alginic acid sodium salt from brown algae; Sigma-Aldrich, St. Louis, MO) in double-distilled water under stirring conditions and at room temperature to form a homogenous solution at a final concentration of 4.0% (w/v).

To analyze the effects of dextran sulfate on simvastatin encapsulation efficiency in chitosan-coated alginate microspheres, microspheres were prepared using alginate alone or mixed with dextran sulfate. In the latter case, different stock solutions of dextran sulfate (molecular weight of approximately 500,000 g/mol, ultra pure grade; Amresco, Solon, OH) were first prepared in double-distilled water at a concentration of 0.67%, 2.00% or 3.35% (w/v) under

stirring conditions and at room temperature. Alginate powder was then added to the dextran sulfate solutions at a concentration of 4.0% (w/v) and stirred thoroughly at room temperature to obtain a homogenous solution.

4.4.4 Microsphere synthesis

The alginate microspheres were synthesized using the external gelation technique as follows. A 300 μL of the previously prepared 4.0% (w/v) alginate solution (without dextran sulfate) was loaded in a 3 mL syringe (Luer-Lok™ Tip, BD Diagnostics, Mississauga, ON). The syringe was then connected to another empty 3 mL syringe via a Poly(vinyl-chloride) (PVC) tubing, which was approximately 1 inch in length. One hundred (100 μL) aliquot of activated simvastatin complexed with HP-βCD (at the highest pre-determined complexation percentage) was then injected in the PVC tubing via a gastight syringe (Hamilton Company, Reno, NV), and the injection site was sealed with paraffin stripes. The solutions were then mixed by pumping the syringes back and forth for approximately 3 minutes in order to obtain a homogenous solution with a final alginate concentration of 3.0% (w/v). After mixing, the solution was kept in only one of the two syringes, which was detached from the PVC tube and attached to a 30 gauge and a half-inch needle (BD PrecisionGlide™ Needle, Franklin Lakes, NJ). The extrusion nozzle was then fixed to the syringe, which was clamped on a custom-made extrusion pump (Figure 4.1). The syringe content was extruded in the previously prepared gelation medium (60 mL; with a distance of approximately 4 cm between the tip of the nozzle and the surface of the gelation medium) composed of 5.0% (w/v) $CaCl_2$ solution with or without 0.1% (w/v) chitosan solution (to analyze the effects of chitosan coating on simvastatin encapsulation efficiency). A polymer flow rate of 30 μL/minute and a coaxial air flow set at 4.0 psi were used in all experiments and the gelation medium was placed under stirring conditions (180 rpm, Corning magnetic stirrer, PC-410D, Corning, NY). After the extrusion, the microspheres were cured in the gelation medium for 15 minutes in order to completely solidify.

To analyze the effects of dextran sulfate on simvastatin encapsulation efficiency in chitosan-coated alginate microspheres, the same procedure as described above was used to synthesize the microspheres, with the exception that the 300 μL of the previously prepared 4.0% (w/v) alginate solution contained 0.67, 2.00, or 3.35% (w/v) dextran sulfate. The extrusion was performed in the previously prepared gelation medium (60 mL) composed of 5.0% (w/v) $CaCl_2$

and 0.1% (w/v) chitosan, using the custom-made extrusion pump. After the extrusion, the microspheres were cured in the gelation medium for 15 minutes in order to completely solidify.

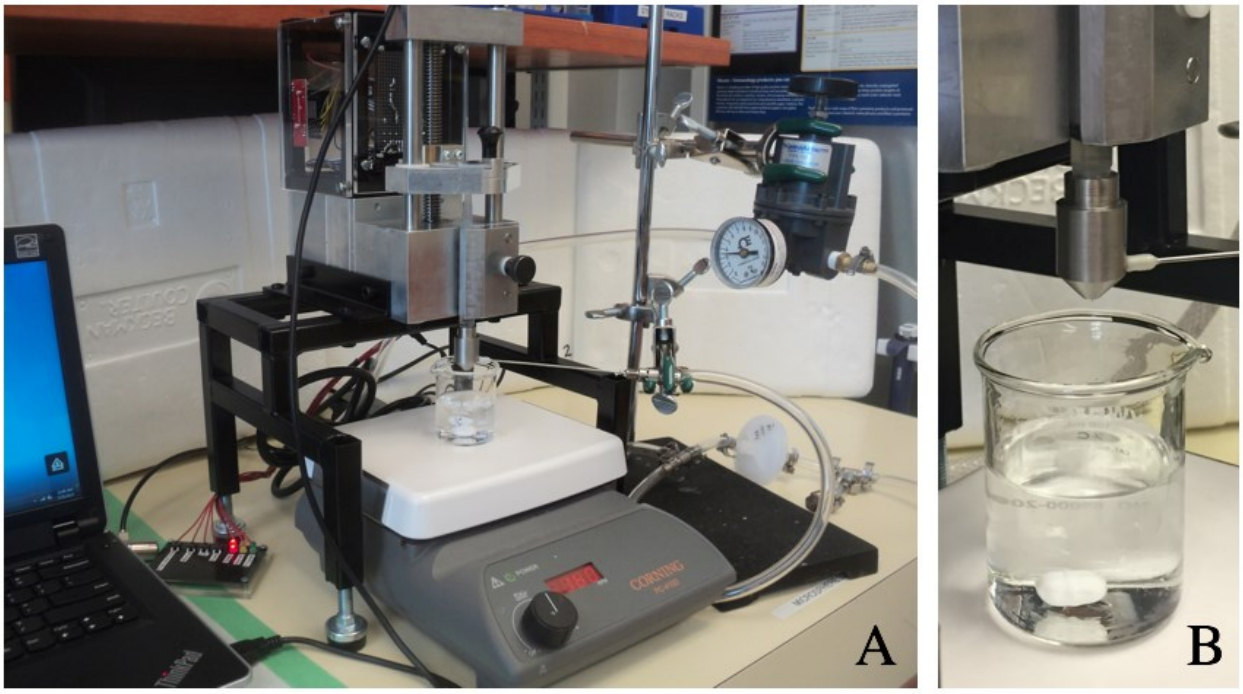

Figure 4.1 Custom-made extrusion pump used to synthesize the microspheres: (A) Overall set-up; (B) Close-up image depicting the extrusion process and showing the syringe nozzle.

The microsphere formulation (with chitosan coating and dextran sulfate) that led to the highest simvastatin encapsulation efficiency (measured as described in the following section) was then selected to optimize the gelation conditions, i.e., the volume of the gelation medium, the curing time and the addition of simvastatin into the gelation medium. First, two additional volumes of gelation medium were tested (30 mL and 20 mL). The volume that led to the highest simvastatin encapsulation efficiency was then selected to analyze the effects of the curing time (15 and 5 minutes), under the assumption that the diffusion of simvastatin from the microspheres into the gelation medium would decrease by decreasing the curing time. The optimum volume of gelation medium and curing time were finally adopted to analyze the effect of the addition of simvastatin into the gelation medium. Activated simvastatin complexed with HP-βCD (0.263 mM simvastatin based on simvastatin maximum solubility, and at the highest pre-determined complexation percentage) was added to the gelation medium, which was then mixed under

stirring conditions (500 rpm) for approximately 5 minutes at room temperature prior to the extrusion process.

4.4.5 Encapsulation efficiency measurements

The synthesized microspheres were filtered using a Falcon cell strainer with a sieve size of 100 μm (Corning Incorporations, Durham, NC) and rinsed three times with 1 mL of double-distilled water to remove any excess of $CaCl_2$ and/or chitosan from the gelation medium. The filtered microspheres were then gently placed in 1 M NaOH with a spatula and magnetically stirred for 24h at room temperature in order to facilitate the breakdown of the cross-linked alginate. After complete dissolution, the resulting solutions were centrifuged at 850 g for 5 minutes, and the absorbance of simvastatin in the supernatants was measured at 238 nm using a hybrid microplate reader, as previously described. Standard curves were prepared in 1 M NaOH using the simvastatin complexed with HP-βCD (same simvastatin-HP-βCD solution used for preparation of the microspheres). Finally, the encapsulation efficiency (%) was determined as the ratio of the simvastatin mass in the microspheres (measured in the solution after complete dissolution of the microspheres) over the initial mass of complexed simvastatin used for the preparation of microspheres.

4.4.6 Microsphere size and morphology analysis

The diameter of 100 microspheres synthesized with the optimum formulation (the one that led to the highest simvastatin encapsulation efficiency) was measured on light microscopy micrographs taken with a Nikon Digital Sight DS-Ri1 camera mounted on a Nikon Eclipse Ti inverted microscope system and using NIS Elements Basic Research imaging software version 3.20.01 and a 10x Plan Fluor objective (Nikon Instruments, Melville, NY). The average diameter was then calculated.

In addition, the surface morphology of the microspheres was analyzed using a cryo-scanning electron microscopy (cryo-SEM; performed at the Carleton University Nano Imaging Facility, Ottawa, ON) (Tescan Vega2 XMU; Tescan, Brno, Czech Republic). Briefly, microspheres were pipetted on a sample holder using a p1000 pipette, and an end-cut pipette tip (approximately 0.5 inch cut with a scissor) in order to avoid damaging the microspheres. The sample holder was then placed in a cryo-chamber and the microspheres were frozen at -60° C

followed by sublimation at -40° C for 15 minutes. The microspheres were finally examined with a back-scatter detector and at an accelerating voltage of 20 kV, at 200x and 350x magnifications.

4.4.7 Statistical analysis

All experiments were performed in triplicate and data are expressed as means ± SD. Statistical analysis was performed using one-way ANOVA and Tukey Kramer tests, with $p<0.05$ considered to be statistically significant.

4.5 Results

4.5.1 Simvastatin complexation with HP-βCD

Results showed that the complexation of simvastatin with HP-βCD increased with increasing HP-βCD to simvastatin molar ratios, up to 97.6% ± 2.5% with a molar ratio of 10 ($p=0.001$, relative to molar ratio of 2) (Figure 4.2). Therefore, this molar ratio was used for the subsequent experiments.

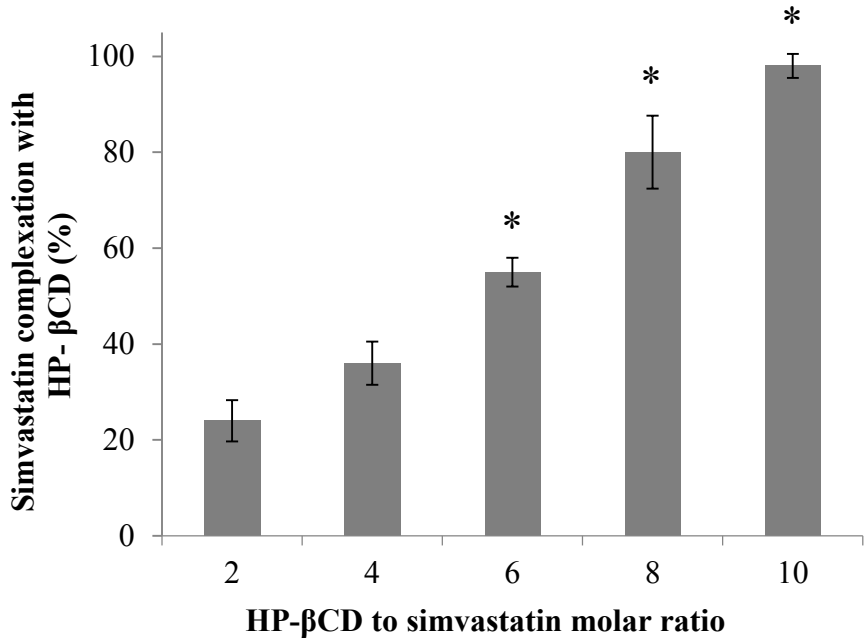

Figure 4.2 Effects of 2-hydroxypropyl-β-cyclodextrin (HP-βCD) to simvastatin molar ratio on simvastatin complexation with HP-βCD. Data are expressed as means ± SD of three experiments. An asterisk (*) indicates a significant difference ($p<0.05$) between a given HP-βCD to simvastatin molar ratio and the molar ratio of 2.

4.5.2 Effects of chitosan on simvastatin encapsulation efficiency

Results showed that simvastatin encapsulation efficiency was negligible in 3.0% (w/v) alginate microspheres synthesized in 5.0% (w/v) $CaCl_2$ solution without chitosan. However, it increased up to 10.6% ± 0.3% with the addition of chitosan ($p<0.001$). Therefore, chitosan-coated alginate microspheres were used for the subsequent experiments.

4.5.3 Effects of dextran sulfate on simvastatin encapsulation efficiency

The addition of 0.67% (w/v) dextran sulfate in 4.0% (w/v) alginate solution (final concentrations in the simvastatin-loaded microspheres: 0.5% (w/v) and 3.0% (w/v), respectively) did not significantly increase simvastatin encapsulation efficiency in chitosan-coated alginate microspheres (Figure 4.3). However, the addition of 2.0% (w/v) dextran sulfate (final concentration of 1.5% (w/v)) increased the encapsulation efficiency up to 14.0% ± 1.2% ($p=0.021$). Interestingly, the addition of 3.35% (w/v) dextran sulfate (final concentration of 2.5% (w/v)) resulted in a decrease in simvastatin encapsulation efficiency down to 8.9% ($p=0.002$ relative to 2.0% (w/v) dextran sulfate). Therefore, the addition of 2.0% (w/v) dextran sulfate was used for the subsequent experiments.

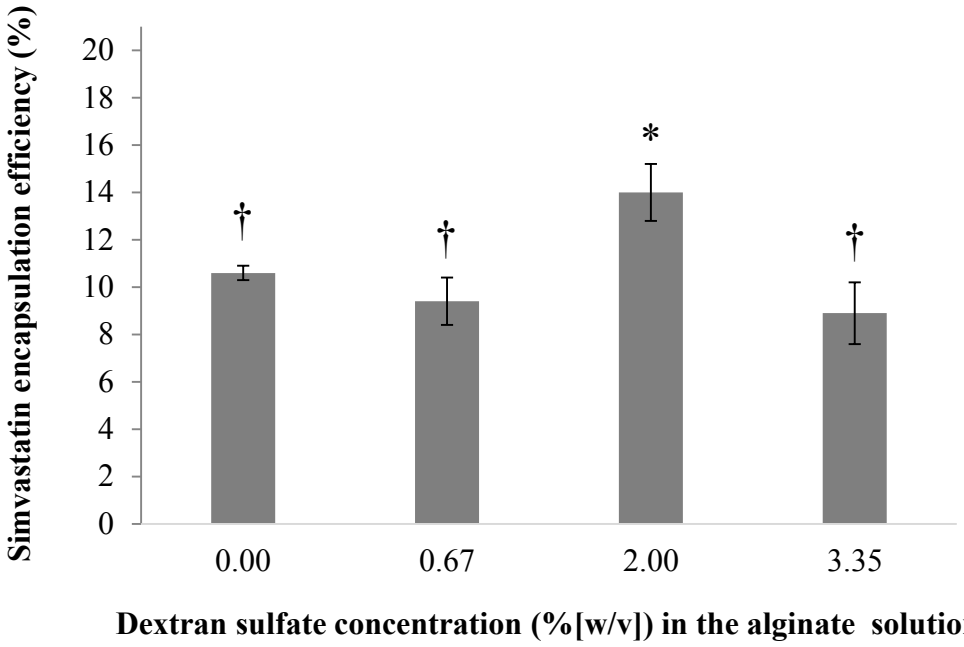

Figure 4.3 Effects of dextran sulfate concentration (%[w/v]) initially added in the alginate solution on simvastatin encapsulation efficiency in the microspheres (%). Data are expressed as means ± SD of three experiments. An asterisk (*) indicates a significant difference ($p<0.05$) between a given dextran sulfate concentration and no dextran sulfate. A dagger (†) indicates a significant difference ($p<0.05$) between a given dextran sulfate concentration and 2.0% (w/v) dextran sulfate.

4.5.4 Effects of gelation conditions on simvastatin encapsulation efficiency

Volume of the gelation medium

Decreasing the volume of the gelation medium from 60 mL to 30 mL or 20 mL did not significantly affect simvastatin encapsulation efficiency in chitosan-coated alginate microspheres containing dextran sulfate (Table 4.1). Therefore, the lowest volume (20 mL) was used for the subsequent experiments.

Table 4.1 Effects of gelation conditions including volume of the gelation medium, curing time, and the addition of simvastatin in the gelation medium, on simvastatin encapsulation efficiency (EE). Data are expressed as means ± SD of three experiments.

Variable	Alginate concentration* (% [w/v])	Dextran sulfate concentration* (% [w/v])	Gelation medium (% [w/v])	Volume of gelation medium (mL)	Curing time (min)	Simvastatin concentration in gelation medium (mM)	EE (%)
Volume of the gelation medium	3.0%	1.5%	5.0% $CaCl_2$ 0.1% chitosan	60	15	0	14.0 ± 1.2
				30			14.2 ± 0.5
				20			14.0 ± 1.2
Curing time	3.0%	1.5%	5.0% $CaCl_2$ 0.1% chitosan	20	15	0	14.0 ± 1.2
					5		15.4 ± 3.3
Addition of simvastatin in the gelation medium	3.0%	1.5%	5.0% $CaCl_2$ 0.1% chitosan	20	5	0	14.0 ± 1.2
						0.263	22.4 ± 1.3

* Final concentrations in the microspheres.

Curing time

Results showed no significant difference in simvastatin encapsulation efficiency when decreasing the gelation time from 15 to 5 minutes (Table 4.1). However, results with the 5-minute curing time showed a higher variability, as depicted by the higher standard deviation. Therefore, the initial 15-minute curing time was maintained for the analysis of the addition of simvastatin into the gelation medium, and for the analysis of microsphere size and morphology.

Addition of simvastatin into the gelation medium

Results showed an increase in simvastatin encapsulation efficiency, up to 22.4% ± 1.3% ($p=0.001$), when the microspheres were synthesized in gelation medium containing simvastatin (Table 4.1). Therefore, gelation medium containing simvastatin was used for the analysis of microsphere size and morphology.

4.5.5 Microsphere size and morphology analysis

Light microscopy analysis of chitosan-coated alginate microspheres containing dextran sulfate (final alginate and dextran sulfate concentrations in the microspheres: 3.0% and 1.5% (w/v), respectively) showed that the microspheres were overall homogeneous and spherical (Figure 4.4), with an average diameter of 328.7 ± 22.0 μm (average of three experiments). Cryo-SEM analysis showed a smooth and regular surface of the chitosan-coated alginate microspheres enriched with dextran sulfate (Figure 4.5).

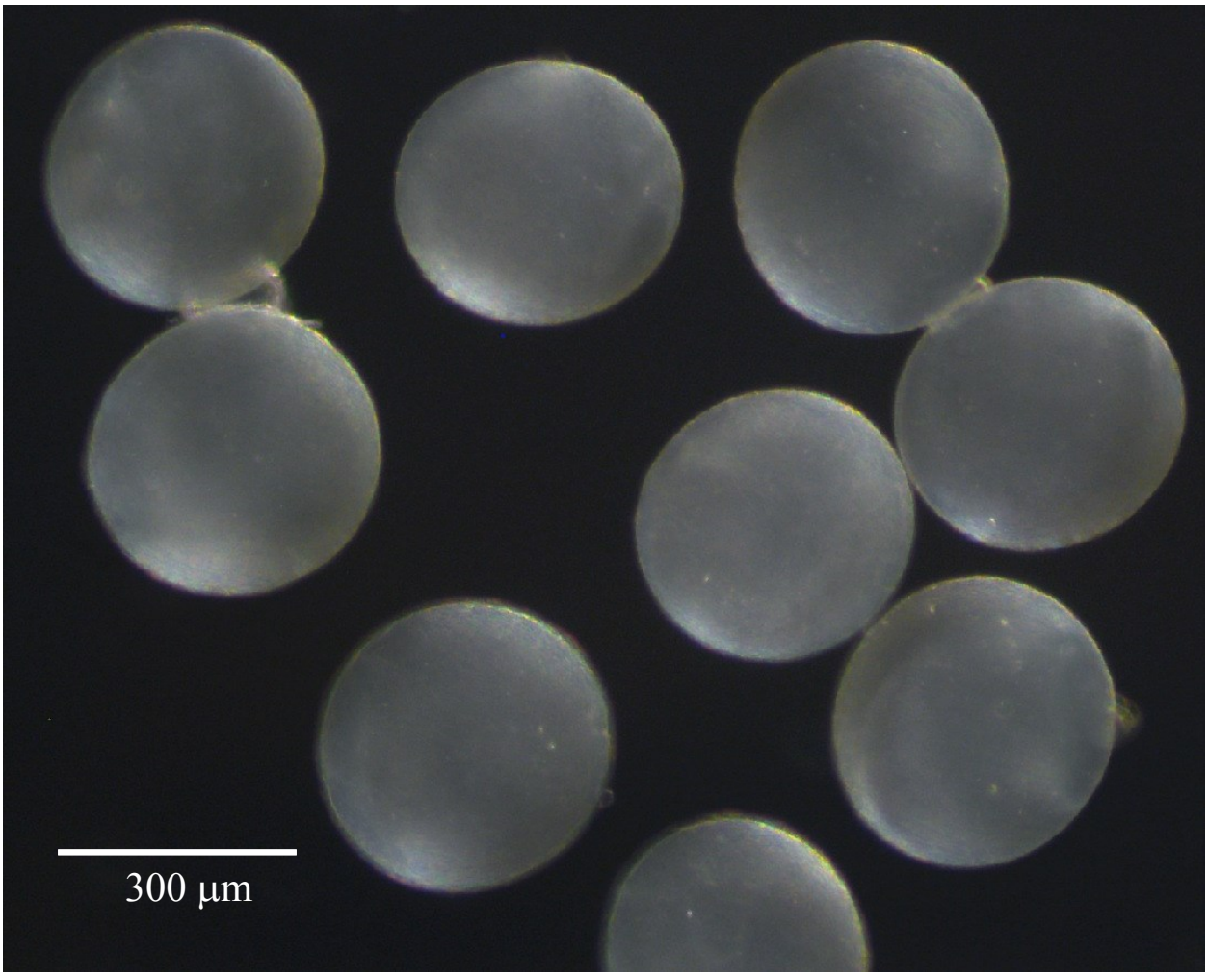

Figure 4.4 Representative light microscopy micrograph of chitosan-coated alginate microspheres containing 1.5% (w/v) dextran sulfate (final concentration in the microspheres).

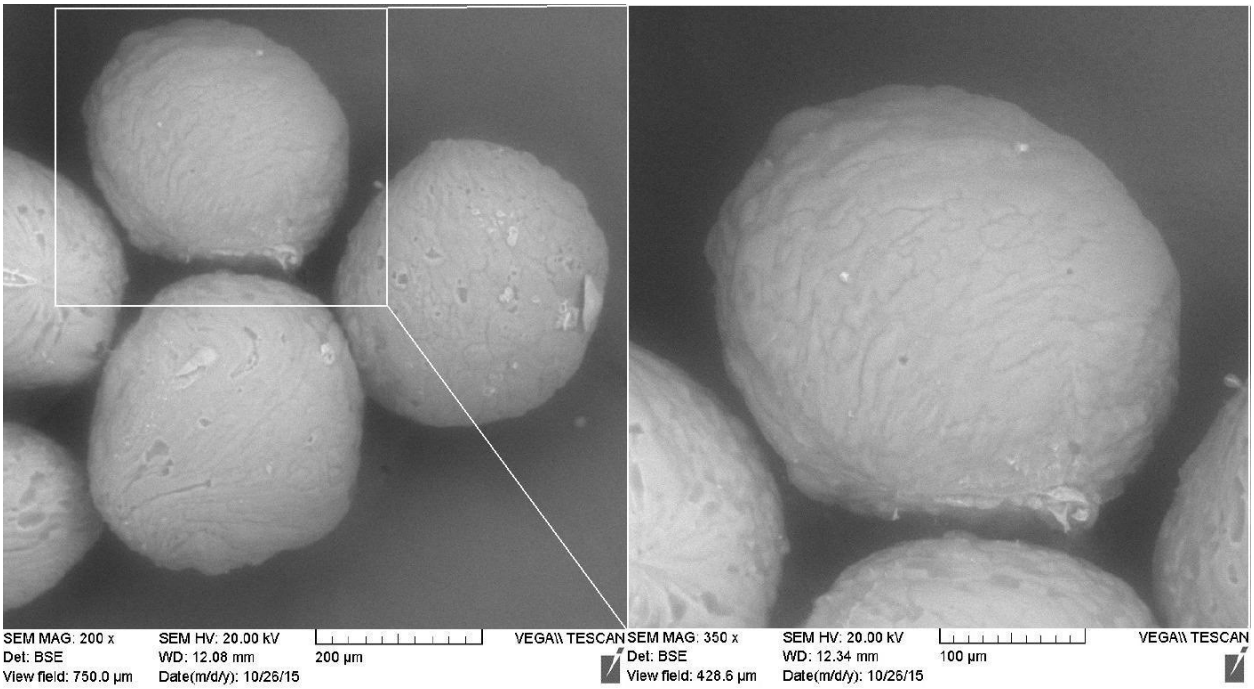

Figure 4.5 Representative cryo-SEM images of chitosan-coated alginate microspheres containing 1.5% (w/v) dextran sulfate (final concentration in the microspheres): A) 200x; and B) 350x magnifications.

4.6 Discussion

Overall, results of the present study showed that simvastatin was successfully complexed with HP-βCD to increase its solubility in alginate solution. Additionally, chitosan coating of the alginate microspheres, along with the combination of alginate with dextran sulfate and the addition of simvastatin in the gelation medium, increased simvastatin encapsulation efficiency, likely by decreasing the diffusion of the drug out of the microspheres during the synthesis.

Alginate microspheres were used in this study as a drug delivery system because of alginate biocompatibility, low toxicity, relatively low cost, and mild gelation conditions [15], [16]. In addition to local drug delivery applications, alginate-based biomaterials have been commonly used in tissue engineering and wound healing as artificial cell scaffolds due to alginate porosity and mechanical strength, which resemble those of the extracellular matrices [15], [149], [202]. Being a polymer approved by the Food and Drug Administration (FDA), alginate is also extensively used in the food industry as an additive as well as gelling and thickening agent [133], [149]. However, two main challenges with the use of alginate

microspheres as a drug delivery system are the difficulty to encapsulate hydrophobic molecules such as simvastatin, and the large microsphere pore size, which can lead to the leakage of low molecular weight drugs [23].

HP-βCD was used in the present study to enhance the stability and solubility of simvastatin in the alginate solution. Indeed, HP-βCD possesses a unique truncated structure with a hydrophilic outer shell and a relatively hydrophobic inner core, which allows the formation of 1:1 stoichiometric inclusion complexes with simvastatin [139], thereby increasing simvastatin solubility and stability in aqueous solutions, as shown in phase solubility studies [139], [140]. The complexation procedure used in the present study, adopted from Yoshinari et al. [142], was followed by the direct measurement of the percentage of simvastatin complexed with HP-βCD, which had not been reported in previous phase solubility studies [139]–[141]. Results showed the highest complexation percentage (97.6%) with a HP-βCD to simvastatin molar ratio of 10. This high complexation percentage may be explained by the low pH of the simvastatin solution (pH 4.2), which is slightly above the pK_a of the carboxylic acid of the lactone ring (pKa=4.18). Indeed, Yoshinari et al. [142] reported a significantly higher complexation percentage of simvastatin with βCD at pH 4.2 (79%) than at pH 6.8 (6%). Interestingly, the maximum complexation percentage of simvastatin with HP-βCD in the present study (97.6%) was higher than the 79% reported by Yoshinari et al., who used βCD. This difference may be explained by a higher solubility of HP-βCD than βCD, the higher molar ratio used in the present study (10) vs. 2 used by Yoshinari et al., as well as differences in the measurement methods. Indeed, Yoshinari et al. considered the precipitated simvastatin as being complexed with βCD, whereas the present study showed that simvastatin complexed with HP-βCD was actually dissolved since simvastatin clearly precipitated in the absence of HP-βCD.

The encapsulation efficiency results showed negligible encapsulation of simvastatin in 3.0% (w/v) alginate microspheres without chitosan, likely because of the large alginate microsphere pore size leading to the diffusion of the drug out of the microspheres during the synthesis process, as suggested by Lee and Mooney [15]. These results corroborate those of Hari et al. [168], who also showed a low encapsulation efficiency (4%) of nitrofurantoin (a low molecular weight drug similar to simvastatin) in 2.0% (w/v) alginate microspheres. The addition of 0.1% (w/v) chitosan in the gelation medium significantly increased simvastatin encapsulation efficiency up to 10.6%, likely by decreasing the loss of the encapsulated drug molecules during

the microsphere synthesis process as well as the washing steps, especially those entrapped close to the microsphere surface. Indeed, the positively-charged amino groups of chitosan and the negatively-charged carboxyl group of alginate form a strong polyelectrolyte complex coating, thereby leading to a denser outer layer with reduced pore size [133], [199]. This is in agreement with other studies that have also reported an increased encapsulation efficiency of other molecules in chitosan-coated alginate microspheres [23], [168], [192], [203], [204].

Dextran sulfate was used as a blending polymer to decrease the pore size of the chitosan-coated alginate microspheres. Results showed a significant increase (up to 14.0%) of simvastatin encapsulation efficiency in the chitosan-coated alginate microspheres containing 1.5% (w/v) dextran sulfate (final concentration in the microspheres). This increase may be explained by the formation of a denser alginate matrix that may delay the diffusion of the drug across the polymer network [205], as well as the formation of stronger electrostatic bonds between the negatively-charged alginate supplemented with dextran sulfate and the positively charged chitosan in the outer layer. This, in turn, would lead to the formation of a denser outer layer [23], helping to retain simvastatin inside the microspheres. These results corroborate those of Khorram et al. [23], who also reported an increase in the encapsulation efficiency of low molecular weight propranolol-HCl with 1.0% (w/v) dextran sulfate in 3.0% (w/v) chitosan-coated alginate microspheres [23]. A higher concentration of dextran sulfate (final concentration of 2.0% [w/v] in the microspheres) resulted in a significant decrease in simvastatin encapsulation efficiency, likely because of the increase in the initial polymer solution viscosity limiting the extrusion procedure and leading to the formation of microspheres with variable size and shape. Therefore, dextran sulfate at the final concentration of 1.5% (w/v) in the microspheres was selected for the subsequent experiments.

The effects of several extrusion parameters including the volume of the gelation medium, the curing time and the addition of simvastatin in the gelation medium were analyzed. Results showed that the volume of the gelation medium (from 60 mL down to 20 mL) did not significantly affect simvastatin encapsulation efficiency. Therefore, the lowest volume of 20 mL was used for the subsequent experiments. The curing time of the microspheres has been shown to be a governing factor in encapsulation efficiency studies [206]–[208]. It should allow the complete hardening of the microsphere post-extrusion, while being minimal in order to avoid drug loss by diffusion during the microsphere synthesis [207]. For example, a study by

Abdelbary et al. [207] reported that chitosan-coated alginate microcapsules required a 10-minute curing time when using 2.0% (w/v) alginate and 0.2 M $CaCl_2$ (equivalent to approximately 2.2% (w/v) $CaCl_2$). On the other hand, Patel et al. [206] and Wong and Chang [208] reported that a 15-minute curing time was required when using 2.0% (w/v) alginate beads prepared with 5.0% (w/v) and 1.0% (w/v) $CaCl_2$, respectively. In the present study, a 15-minute vs. 5-minute curing time did not significantly affect simvastatin encapsulation efficiency, although the 5-minute led to a higher variability in the results, as depicted by the higher standard deviation. Therefore, the initial 15-minute gelation time was used subsequently. Finally, the addition of simvastatin into the gelation medium (at 0.263 mM based on the maximum solubility) significantly increased simvastatin encapsulation efficiency up to 22.4%, likely due to a decreased concentration gradient of simvastatin between the microspheres and the gelation medium, leading to a decrease in the diffusion of simvastatin out of the microspheres.

Overall, the maximum encapsulation efficiency of simvastatin obtained in this study still remains rather lower compared to other studies. For example, Tai et al. [130] reported a 77.7% encapsulation of simvastatin in poly(lactic-co-glycolic acid)/hydroxyapatite (PLGA/HAp) microspheres prepared with the water-in-oil-in-water (w/o/w) double emulsion technique. The differences in the encapsulation efficiencies could be due to the hydrophobicity of PLGA solution, favourable to simvastatin that is also hydrophobic. In the present study, the hydrophobicity of simvastatin was compensated by its complexation with HP-βCD. However, it is possible that this initial complexation was partially lost during the extrusion process, leading to a leakage of the hydrophobic simvastatin from the microspheres. Nevertheless, the differences in the encapsulation efficiencies may also be explained by differences in the measurement methods. Indeed, in the present study, the alginate microspheres were dissolved in 1 M NaOH solution, allowing the gradual replacement of the Ca^{2+} ions by Na^{+} ions, and thereby facilitating the break-up of the alginate chains. This allowed a direct measurement of the simvastatin content inside the microspheres, giving a more precise encapsulation efficiency. In contrast, in the study from Tai et al. [130], as in many other encapsulation studies reported in the literature [23], [164], [169], [176], the encapsulation efficiency was measured by subtracting the amount of non-encapsulated drug in the gelation medium from the initial amount of drug used. This indirect method may lead to an overestimation of the encapsulated drug since it only accounts for the amount of drug loss in the final stage of the encapsulation procedure [177], and does not account

for the extrusion process (prior to the microsphere formation in the gelation medium the mass of the drug left in the experimental apparatus (e.g., syringes, containers, etc.) or degraded during the synthesis process prior to the microsphere formation in the gelation medium. For example, Khorram et al. [23] reported a 70.8% encapsulation efficiency of the low molecular weight propranolol-HCl in 3.0% (w/v) alginate microspheres coated with 0.5% (w/v) chitosan, and supplemented with 1.0% (w/v) dextran sulfate. Their release kinetic studies showed that only about 50% of the encapsulated drug was released. However, the authors did not determine if the sum of the remaining mass of the drug inside the microspheres together with the mass of the released drug was equal to the expected encapsulated mass.

4.7 Conclusion

The complexation procedure developed in the present study resulted in a high complexation percentage of simvastatin with HP-βCD, which should increase the solubility of simvastatin in alginate, and thereby facilitate its encapsulation in the microspheres. Furthermore, chitosan-coating of the alginate microspheres as well as the addition of 2.0% (w/v) dextran sulfate in the alginate solution significantly improved simvastatin encapsulation efficiency. Finally, the addition of simvastatin in the gelation medium further increased the encapsulation efficiency, likely by decreasing the diffusion of simvastatin from the microspheres into the gelation medium. Nevertheless, the maximum encapsulation efficiency still remains rather low. Future studies should therefore include additional strategies to further decrease simvastatin diffusion out of the microspheres, with, for example, the addition of an extra coating layer and/or blending polymers in the alginate in order to form a denser polymer matrix.

4.8 Acknowledgements

This study was supported by the Canada Research Chairs Program and the Canadian Institutes of Health Research (CIHR). The authors thank Dr. Mehrdad Rafat for the early development of the extrusion process, Matthieu Lemay for designing the extrusion pump, Stephen J. Baskey for designing the extrusion nozzle, and Adrien Moya for preliminary optimization of the extrusion parameters.

5 Thesis Discussion

5.1 Conclusions from the Work

This thesis represents the initial steps for the development of a drug delivery system made of alginate-based microspheres for local release of simvastatin. The manuscript included in this thesis describes different strategies to improve the encapsulation efficiency of simvastatin in the alginate microspheres, and the results fulfill the two specific objectives of this thesis, i.e.: 1. To complex simvastatin with 2-hydroxypropyl-β-cyclodextrin (HP-βCD) in order to increase its solubility; and 2. To increase simvastatin encapsulation efficiency in alginate microspheres by coating the microspheres with chitosan, adding dextran sulfate to the alginate solution, and optimizing the gelation conditions used for the synthesis of the microspheres (e.g., volume of the gelation medium, curing time, and addition of simvastatin in the gelation medium).

For the first objective, simvastatin was complexed with HP-βCD using a complexation procedure adapted from Yoshinari et al. [142]. Results showed that simvastatin complexation with HP-βCD increased with HP-βCD to simvastatin molar ratio, to a maximum of 97.6% with the molar ratio of 10. This finding is both novel and significant as it led to a very high complexation percentage of simvastatin with HP-βCD that should increase the solubility of simvastatin in alginate microspheres, and thereby facilitate its encapsulation.

The results pertaining to the second objective demonstrated that chitosan-coating of the alginate microspheres significantly increased simvastatin encapsulation efficiency, which was further increased by the addition of 2.0% (w/v) dextran sulfate in the alginate solution. Results also showed that the addition of simvastatin in the gelation medium significantly increased simvastatin encapsulation efficiency while the volume of the gelation medium and the curing time did not have any significant effect. Together, these results showed that a combination of polymers and optimized gelation conditions were effective in improving simvastatin encapsulation efficiency, likely by counteracting the diffusion of simvastatin out of the microspheres.

5.2 Technical Considerations

5.2.1 Optimization of the extrusion parameters

The initial stages of this work involved many pilot experiments to optimize the extrusion parameters, including the volume ratio of simvastatin to alginate solution (containing or not dextran sulfate), as well as the polymer flow rate and air flow pressure set on the extrusion pump. Different volume ratios of simvastatin (μL) to alginate solution (μL) were tested (50:350, 100:300, and 200:200), with the final extrusion volume of the mixture fixed at 400 μL. The optimum volume ratio of simvastatin to alginate solution was determined to be 100:300, since the 50:350 ratio led to a lower simvastatin encapsulation efficiency, and the 200:200 ratio led to a compromised homogeneity of the extrusion process because of the higher dilution of the alginate solution. The resulting heterogeneity of the microspheres may have been due to the impaired cross-linking process of the more diluted alginate solution, or the adverse effects of the NaOH and/or ethanol component of the activated simvastatin on the alginate integrity.

With regards to the polymer flow rate and air flow pressure, it is important to note that these two parameters have complementary effects on the formation of the microspheres. The alginate solution should be extruded using an optimum polymer flow rate and air flow pressure to form microspheres with a homogeneous size and shape. In this work, the flow rate was pre-set at 30 μL/min (based on previous experiments conducted by other students) and initially paired with various air flow pressures (3, 3.5, 4 and 4.5 psi). The homogeneity of the microspheres in terms of size and shape was then analyzed for each experiment using light microscopy. Based on the results, the air flow pressure of 4 psi was determined to be optimum. Because the polymer flow rate and the air flow pressure have synergic effects, if the air flow was to be decreased in future work, the polymer flow rate would have to be increased, and vice-versa.

5.2.2 Measurements of potential losses of simvastatin in the experimental set-up

Prior to dissolving the microspheres to measure simvastatin encapsulation efficiency, the extruded microspheres in the gelation medium were filtered using a Falcon cell strainer (Corning Incorporations, Durham, NC), with a sieve size of 100 μm, and then washed three times with 1 mL of water in order to remove any traces of $CaCl_2$ and/or chitosan. The use of a cell strainer allowed the water used for each wash to quickly pass through the filter and get absorbed using paper wipers (Kimwipes®) placed along the walls and the bottom of the cell strainer. The loss of

encapsulated simvastatin during this process was minimal. Indeed, ancillary encapsulation efficiency experiments that included the measurement of simvastatin in the washes by UV absorbance reading at 238 nm (in this case, the water used for the washes was pipetting out instead of being absorbed on the paper wipers) showed a minimal amount of simvastatin in the first wash solution, likely from traces of the gelation medium left on the surface of the microspheres, and a negligible amount in the second and third washes.

Finally, the amount of simvastatin left behind in the extrusion syringe was also measured by washing the syringe three times with 1 mL of water and measuring the simvastatin absorbance in the washes. Results showed that about 20% of the initial amount of simvastatin was left in the syringe at the end of the experiment.

5.2.3 Preliminary release kinetics experiments

Preliminary release kinetic studies using the optimum microsphere formulation (i.e., chitosan-coated alginate microspheres with dextran sulfate, prepared with the addition of simvastatin in the gelation medium) were performed in SBF. For these experiments, the washed microspheres (as described above in Section 5.2.2 for the encapsulation efficiency experiments) were gently scooped using a metal spatula and transferred into a 20 mL PET glass liquid scintillation vial (Wheaton, Millville, NJ) containing 3 mL of SBF (prepared following the protocol of Kokubo and Takadama [209]). A 600 μL aliquot of the SBF solution (divided into three aliquots of 200 μL) was pipetted out after 5 minutes following a gentle swirl of the glass bottle, and the amount of simvastatin released in the SBF solution was measured in the three aliquots by UV absorbance at 238 nm. The SBF aliquots were then pipetted back into the glass bottle (this method was used instead of replenishing the glass bottle with fresh SBF to avoid removing simvastatin from the samples at each time point). Absorbance readings were performed every 5 minutes up to 30 minutes and every 30 minutes thereafter for up to two hours. Results (from 3 experiments) showed a rapid release of simvastatin (approximately 80% of the encapsulated simvastatin) within 15 minutes, which then reached a plateau (likely due to the equilibrium reached between the concentration of simvastatin in the microspheres and in the SBF solution).

The use of 1 mL of SBF (instead of 3 mL) was also tested (3 experiments were performed). In this case, the washed microspheres were scooped into a 2-mL siliconized low

retention microcentrifuge tube containing 1 mL of SBF (because of the smaller SBF volume, a microcentrifuge tube had to be used instead of a 20 mL PET glass liquid scintillation vial, so that the 1 mL of SBF would cover all the microspheres). Absorbance readings were performed every 5 minutes (as for the 3-mL volume experiments), but using a NanoDrop spectrophotometer (Thermo Scientific NanoDrop ND-2000c Spectrophotometer). Results showed that approximately 35% of the encapsulated simvastatin was released within 15 minutes, after which the release reached a plateau, similarly to what was observed when using 3 mL of SBF. Overall, results with 3 and 1 mL of SBF suggest that simvastatin release was primarily governed by diffusion.

Finally, at the end of the release kinetic studies (using either 3 mL or 1 mL of SBF), the SFB solution was replaced with 1 mL of fresh SBF to induce the release of the remaining simvastatin inside the microspheres. Absorbance reading was performed after 15 minutes. In both cases, the measured amount of simvastatin together with the amount released during the kinetic studies matched the simvastatin amount initially encapsulated.

5.3 Future Studies

5.3.1 Simvastatin encapsulation efficiency

The results of this thesis project suggest that the increase of simvastatin encapsulation efficiency in alginate microspheres through the use of chitosan coating and dextran sulfate as well as the addition of simvastatin in the gelation medium was likely due to a decrease in the diffusion of simvastatin out of the microspheres. However, based on the encapsulation efficiency results (still rather low) and preliminary results of the release kinetics (as discussed in section 5.2.3), the pore size of the alginate-dextran sulfate microspheres appears to remain rather large for the entrapment of simvastatin, even when using the highest alginate and dextran sulfate concentrations (final concentrations of 3.0% (w/v) alginate and 1.5% (w/v) dextran sulfate in the microspheres). Therefore, future studies could consider additional strategies to further decrease the diffusion of simvastatin. For example, several studies have used high molecular weight carbohydrates such as pectin [210]–[212] and methylcellulose [213] as a blending polymer with alginate in order to decrease the pore size of the resulting gel. Thus, the use of pectin and/or methycellulose (in addition to or instead of dextran sulfate) could also be considered to further improve simvastatin encapsulation efficiency. In addition, when incorporating new polymers,

there may be a need to further adjust/optimize several extrusion parameters due to changes in the properties of the polymer solution in order to synthesize homogenous microspheres in terms of size and shape. For example, the polymer flow rate, the air flow pressure, and the distance between the nozzle and the surface of the gelation medium affect the size and the shape of the microspheres, such that a too low flow rate and too low air flow as well as a too large distance between the nozzle and the surface of the gelation medium would result in the formation of tear-dropped and larger microspheres.

Another approach to decrease the permeability of the chitosan-coated alginate microspheres could be via the addition of other cross-linking agents (in addition to calcium) such as carbodiimide or glutaraldehyde in the gelation medium, which have been suggested to immobilize the encapsulated agents [172]. For example, a study by Maiti et al. [22] showed that the partially oxidized alginate chains with sodium metaperiodate allowed additional covalent cross-linking sites with adipic acid dihydrazide (ADH), which was added to the gelation medium. This enhanced cross-linking resulted in an encapsulation efficiency of a low molecular weight drug (similar to simvastatin) up to 89%. It also allowed a sustained and complete release of the encapsulated drug over a period of almost 8 hours from ADH-treated oxidized alginate beads compared to 1 hour and a half from untreated oxidized beads, when using a buffer solution with a physiological pH [22]. The authors suggested that the presence of ADH in the gelation medium created a strong membrane in the periphery of the alginate beads that acted as a barrier against the drug diffusion. Other coating layers such as poly(L-lysine) [157], [214], [215], polyvinyl amine [216], [217] silk fibroin [218] and polyethylene glycol [172] have also been used in several studies to reduce the permeability of alginate-based microspheres, thereby minimizing the loss of encapsulated pharmaceutical agents. Therefore, the effects of polycationic agents as alternatives to chitosan or additional coating layers could be analyzed on the encapsulation efficiency of simvastatin.

Finally, a ‘dual ionic and photo cross-linking’ technique was recently suggested to be a promising approach to increase the cross-linking density of the gel matrix [219], which may consequently decrease the pore size of the alginate microspheres. Indeed, in a study by Samorezov et al. [219], alginate microspheres were functionalized with methacrylate groups, which allowed the covalent cross-linking of the chains via free radical polymerization using ultra violet light and a photo-initiator in addition to the conventional calcium cross-linking.

Furthermore, since the methacrylated alginate chains also possess carboxyl groups, the free/remaining methacrylated groups can further cross-link with calcium after photo cross-linking. Therefore, the combination of ionic and covalent bonding, which was shown to enhance stiffness and decrease the swelling of the alginate matrix [219], could also be explored in future studies.

5.3.2 Release kinetics

As explained in Section 5.2.3., preliminary experiments using chitosan-coated alginate microspheres containing dextran sulfate and prepared with the addition of simvastatin in the gelation medium showed that the release of simvastatin in SBF was very rapid (burst release within the first 15 minutes). The magnitude of the initial burst release varied depending on the volume of SFB used, suggesting that the release of simvastatin was primarily governed by diffusion. Therefore, several strategies in combination with the ones mentioned in the previous section (5.3.1) could be adopted to decrease the rapid diffusion of simvastatin from the synthesized microspheres and allow a prolonged release. For example, a study by Valente et al. [147] showed that the encapsulation of bovine serum albumin (BSA)-loaded dextran sulfate-chitosan nanoparticles in alginate microspheres provided an extended release of BSA when compared to the BSA-loaded alginate microspheres. Even though the molecular weight of BSA is much higher than simvastatin (66,000 g/mol vs 418.6 g/mol), a similar system could help obtaining a higher encapsulation efficiency and slowing down the release of simvastatin. Furthermore, the inclusion of the nano-scaled simvastatin-loaded nanoparticles into alginate microspheres may also allow the delivery of multiple drugs. Therefore, future work could focus on developing a dual nano-micro drug delivery system to overcome the large pore size of the alginate microspheres and slow down the release of simvastatin.

Another approach could be to functionalize the alginate chains and HP-βCD via cysteine [220], cysteamine [221] or simply with thiol groups [222] in order to form disulfide bindings between simvastatin-HP-βCD molecules and the alginate chains, assuming simvastatin and HP-βCD remain complexed inside the microspheres during the microsphere synthesis. It would therefore be critical to first determine whether the released simvastatin molecules are still complexed with HP-βCD. Preliminary experiments using size exclusion chromatography with two different flow rates (200 and 400 μL/min) and two different volume fractions (200 μL and

500 μL) were inconclusive as the complexed simvastatin-HP-βCD molecules may dissociate in the chromatography column (Sephadex G-10 MidiTrap, GE Healthcare, bed volume of 5.3 mL). The lack of a reliable control experiment was a limiting factor for the use of size exclusion chromatography. The use of high-performance liquid chromatography electrospray ionization technique should therefore be considered for future studies.

5.3.3 *In vitro* cell culture and *in vivo* animal models

Future *in vitro* studies should include the analysis of the anti-inflammatory effects of simvastatin released from the microspheres to verify its bioactivity once released. More specifically, microspheres could be placed in cultures of macrophages with implant wear particles or metal ions, followed by TNF-α measurement in the culture supernatants in the presence and absence of microspheres. For these experiments, microspheres would need to be sterile. This implies sterilizing the microspheres after their synthesis or performing the synthesis in a sterile environment, using sterile materials and solutions. In either case, it is paramount to adopt an appropriate sterilization method for the selected polymers. Indeed, sterilization may affect the preservation of the polymer integrity as well as the pore size of the cross-linked polymer matrix by altering the mechanical property and/or water retention of the polymer [223]. A study by Stoppel et al. [223] showed that the sterilization of alginate hydrogel via ethanol washing was the most effective method in terms of preserving the mechanical properties and water retention of the alginate hydrogel as well as eliminating bacterial growth, compared to autoclaving and ultra violet light (which may damage the polymer). However, there is a concern regarding the release of simvastatin in the ethanol washes. Alternatively, filtration of the alginate solution (prior to the microsphere synthesis) could be implemented as performed in several studies [224]–[226]. However, possibilities of polymer chain shear, and incomplete filtration of the polymer (due to clogging of the filter pores) may present challenges to maintain the initial concentration of the alginate solution.

Finally, the functionalization of the polymer chains could be a main focus for both *in vitro* and *in vivo* studies to allow specific cell targeting (e.g., macrophages) and enabling the attachment of a fluorescent probe for *in vivo* imaging in small animal models. Indeed, several chemical modifications can be made through the hydroxyl and carboxyl groups of alginate [22]. For instance, the carboxyl groups of alginate have been covalently bound to various fluorescent

probes, out of which fluorochrome fluoresceinamine [227], [228], and protoporphyrin [229] may be promising fluorescent labels to be used for future *in vivo* studies. Alternatively, the amino groups of chitosan could be covalently conjugated with fluorescein isothiocyanate (FITC) as described in the study by Huang et al. [230], who tracked the uptake of the FITC-chitosan nanoparticles in the human epithelium cells.

6 References

[1] K. Ren, A. Dusad, Y. Zhang, and D. Wang, "Therapeutic intervention for wear debris-induced aseptic implant loosening," *Acta Pharm. Sin. B*, vol. 3, no. 2, pp. 76–85, 2013.

[2] K. E. Alvarez, "Total hip replacement," in *New materials and technologies for healthcare*, L. L. Hench, J. R. Jones, and M. B. Fenn, Eds. London, UK: Imperial College Press, 2012, pp. 179–192.

[3] Canadian Institute for Health Information, "Hip and Knee Replacements in Canada: Canadian Joint Replacement Registry 2013 Annual Report," pp. 1–94, 2013.

[4] P. Revell, "The combined role of wear particles, macrophages and lymphocytes in the loosening of total joint prostheses," *J. R. Soc. Interface*, vol. 5, no. 28, pp. 1263–1278, 2008.

[5] G. Holt, C. Murnaghan, J. Reilly, R. M. D. Meek, and S. Features, "The biology of aseptic osteolysis," *Clin. Orthop. Relat. Res.*, vol. 460, no. 460, pp. 240–52, 2007.

[6] I. Catelas and J. J. Jacobs, "Biologic activity of wear particles," *Instr. Course Lect.*, vol. 59, pp. 3–16, 2010.

[7] N. J. Hallab and J. J. Jacobs, "Biologic effects of implant debris," *Bull. NYU Hosp. Jt. Dis.*, vol. 67, no. 2, pp. 182–188, 2009.

[8] G. Mundy, R. Garrett, S. Harris, J. Chan, D. Chen, G. Rossini, B. Boyce, M. Zhao, and G. Gutierrez, "Stimulation of bone formation in vitro and in rodents by statins," *Science*, vol. 286, no. 5446, pp. 1946–1949, 1999.

[9] G. Weitz-Schmidt, "Statins as anti-inflammatory agents," *Trends Pharmacol. Sci.*, vol. 23, no. 10, pp. 482–486, 2002.

[10] F. von Knoch, A. Heckelei, C. Wedemeyer, G. Saxler, G. Hilken, F. Henschke, F. Löer, and M. von Knoch, "The effect of simvastatin on polyethylene particle-induced osteolysis," *Biomaterials*, vol. 26, no. 17, pp. 3549–55, 2005.

[11] A. Hughes, M. J. Rogers, A. I. Idris, and J. C. Crockett, "A comparison between the effects of hydrophobic and hydrophilic statins on osteoclast function in vitro and ovariectomy-induced bone loss in vivo," *Calcif. Tissue Int.*, vol. 81, no. 5, pp. 403–413, 2007.

[12] S. J. Baskey, P. E. Beaulé, E. A. Lehoux, and I. Catelas, "Simvastatin modulates the release of TNF-α and CC chemokines from macrophages exposed to trivalent chromium ions," *J. Biomater. Tissue Eng.*, vol. 4, no. 11, pp. 981–991, 2014.

[13] A. Chaturvedula, M. E. Sale, and H. Lee, "Genetic algorithm guided population pharmacokinetic model development for simvastatin, concurrently or non-concurrently co-administered with amlodipine," *J. Clin. Pharmacol.*, vol. 54, no. 2, pp. 141–149, 2014.

[14] J. Chou, T. Ito, D. Bishop, M. Otsuka, B. Ben-Nissan, and B. Milthorpe, "Controlled release of simvastatin from biomimetic β-TCP drug delivery system," *PLoS One*, vol. 8, no. 1, pp. 2–7, 2013.

[15] K. Y. Lee and D. J. Mooney, "Alginate: properties and biomedical applications," *Prog. Polym. Sci.*, vol. 37, no. 1, pp. 106–126, 2012.

[16] F. Sarei, N. M. Dounighi, H. Zolfagharian, P. Khaki, and S. M. Bidhendi, "Alginate nanoparticles as a promising adjuvant and vaccine delivery system," *Indian J. Pharm. Sci.*, vol. 75, no. 4, pp. 442–9, 2013.

[17] W. R. Gombotz and S. F. Wee, "Protein release from alginate matrices," *Adv. Drug Deliv. Rev.*, vol. 31, no. 3, pp. 267–285, 1998.

[18] O. Jeon, D. S. Alt, S. M. Ahmed, and E. Alsberg, "The effect of oxidation on the degradation of photocrosslinkable alginate hydrogels," *Biomaterials*, vol. 33, no. 13, pp. 3503–14, 2012.

[19] P. Prang, R. Müller, A. Eljaouhari, K. Heckmann, W. Kunz, T. Weber, C. Faber, M. Vroemen, U. Bogdahn, and N. Weidner, "The promotion of oriented axonal regrowth in the injured spinal cord by alginate-based anisotropic capillary hydrogels," *Biomaterials*, vol. 27, pp. 3560–3569, 2006.

[20] C. Gao, M. Liu, J. Chen, and X. Zhang, "Preparation and controlled degradation of oxidized sodium alginate hydrogel," *Polym. Degrad. Stab.*, vol. 94, no. 9, pp. 1405–1410, 2009.

[21] P. Li, Y.-N. Dai, J.-P. Zhang, A.-Q. Wang, and Q. Wei, "Chitosan-alginate nanoparticles as a novel drug delivery system for nifedipine," *Int. J. Biomed. Sci.*, vol. 4, no. 3, pp. 221–8, 2008.

[22] S. Maiti, K. Singha, S. Ray, P. Dey, and B. Sa, "Adipic acid dihydrazide treated partially oxidized alginate beads for sustained oral delivery of flurbiprofen," *Pharm. Dev. Technol.*, vol. 14, no. 5, pp. 461–470, 2009.

[23] M. Khorram, M. Samimi, A. Samimi, and H. Moghadam, "Electrospray preparation of propranolol-loaded alginate beads: Effect of matrix reinforcement on loading and release profile," *J. Appl. Polym. Sci.*, vol. 132, no. 4, p. DOI:[10.1002/app.41334], 2015.

[24] N. Berryman Reese and W. D. Bandy, *Joint range of motion and muscle length testing*, 2nd ed. St. Louis, Missouri: Elsevier Inc., 2010.

[25] K. S. Clippinger, *Dance anatomy and kinesiology*, 2nd ed. Champaigne, Illinois: Human Kinetics, 2007.

[26] "American Academy of Orthopaedic Surgeons," 2010. [Online]. Available: http://www.orthoinfo.org/topic.cfm?topic=A00572. [Accessed: 03-Nov-2015].

[27] M. M. Groh and J. Herrera, "A comprehensive review of hip labral tears," *Curr. Rev. Musculoskelet. Med.*, vol. 2, no. 2, pp. 105–17, 2009.

[28] S. MacDonald, *Getting hip: Recovery from a total hip replacement*. Bloomington, Indiana: AuthorHouse, 2004.

[29] R. Klapper and L. Huey, *Heal your knees: How to prevent knee surgery and what to do if you need it*, 1st ed. Plymouth, UK: The Rowman & Littlefield Publishing Group, 2007.

[30] E. Arden, N. K. Arden, and D. Hunter, *Osteoarthritis*, New York: Oxford University Press Inc, 2008.

[31] L. P. Zebala, P. L. Schoenecker, and J. C. Clohisy, "Anterior femoroacetabular impingement: a diverse disease with evolving treatment options," *Iowa Orthop. J.*, vol. 27, pp. 71–81, 2007.

[32] D. J. Hunter, D. Prieto-Alhambra, and N. Arden, *Osteoarthritis: The facts*, 2nd ed. NYC, NY: The Oxford University Press, 2014.

[33] J. W. J. Bijlsma, F. Berenbaum, and F. P. J. G. Lafeber, "Osteoarthritis: An update with relevance for clinical practice," *Lancet*, vol. 377, no. 9783, pp. 2115–2126, 2011.

[34] G. Peat, R. McCarney, and P. Croft, "Knee pain and osteoarthritis in older adults: a review of community burden and current use of primary health care," *Ann. Rheum. Dis.*, vol. 60, pp. 91–97, 2001.

[35] L. Pulido and C. Restrepo, “Late instability following total hip arthroplasty,” *Clin. Med. Res.*, vol. 5, no. 2, pp. 139–142, 2007.

[36] P. E. Beaulé, D. J. Allen, J. C. Clohisy, P. L. Schoenecker, M. Leunig, and P. E. Beaule, “The young adult with hip impingement: deciding on the optimal intervention,” *Instr. Course Lect.*, vol. 58, pp. 213–222, 2009.

[37] E. W. Paxton, M. Inacio, T. Slipchenko, and D. C. Fithian, “The kaiser permanente national total joint replacement registry,” *Perm. J.*, vol. 12, no. 3, pp. 12–16, 2008.

[38] M. S. McGrath, D. R. Marker, T. M. Seyler, S. D. Ulrich, and M. A. Mont, “Surface replacement is comparable to primary total hip arthroplasty,” *Clin. Orthop. Relat. Res.*, vol. 467, no. 1, pp. 94–100, 2009.

[39] S. M. Kurtz, K. L. Ong, E. Lau, M. Widmer, M. Maravic, E. Gómez-Barrena, M. De Fátima De Pina, V. Manno, M. Torre, W. L. Walter, R. De Steiger, R. G. T. Geesink, M. Peltola, and C. Röder, “International survey of primary and revision total knee replacement,” *Int. Orthop.*, vol. 35, no. 12, pp. 1783–1789, 2011.

[40] W. L. Healy, S. Sharma, B. Schwartz, and R. Iorio, “Athletic activity after total joint arthroplasty,” *J. Bone Joint Surg. Am.*, vol. 90, pp. 2245–2252, 2008.

[41] “Hip Resurfacing,” *Mayo Foundation for Medical Education and Research*, 2015. [Online]. Available: http://www.mayoclinic.org/hip-resurfacing/img-20008999. [Accessed: 03-Nov-2015].

[42] M. Topolovec, A. Cör, and I. Milošev, “Metal-on-metal vs. metal-on-polyethylene total hip arthroplasty tribological evaluation of retrieved components and periprosthetic tissue,” *J. Mech. Behav. Biomed. Mater.*, vol. 34, pp. 243–252, 2014.

[43] N. Hallab and S. Anderson, “Lymphocyte responses in patients with total hip arthroplasty,” *J. Orthop. Res.*, vol. 23, no. 2, pp. 384–391, 2005.

[44] H.-G. Willert, G. H. Buchhorn, A. Fayyazi, R. Flury, M. Windler, G. Köster, and C. H. Lohmann, “Metal-on-metal bearings and hypersensitivity in patients with artificial hip joints. A clinical and histomorphological study,” *J. Bone Joint Surg. Am.*, vol. 87, no. 1, pp. 28–36, 2005.

[45] D. J. Langton, S. S. Jameson, T. J. Joyce, N. J. Hallab, S. Natu, and a V. F. Nargol, "Early failure of metal-on-metal bearings in hip resurfacing and large-diameter total hip replacement: A consequence of excess wear," *J. Bone Joint Surg. Br.*, vol. 92, no. 1, pp. 38–46, 2010.

[46] Y. Abu-Amer, I. Darwech, and J. C. Clohisy, "Aseptic loosening of total joint replacements: mechanisms underlying osteolysis and potential therapies," *Arthritis Res. Ther.*, vol. 9, pp. 1–7, 2007.

[47] J. Gallo, P. Kamínek, V. Tichá, P. Riháková, and R. Ditmar, "Particle disease. A comprehensive theory of periprosthetic osteolysis: a review," *Biomed. Pap.*, vol. 146, no. 2, pp. 21–8, 2002.

[48] O. Furnes, I. L. Havelin, and B. Espehaug, "Properties of bone cement: Which cement should we choose for primary THA?," in *The well-cemented total hip arthroplasty: theory and practice*, S. Breusch and H. Malchau, Eds. Springer, 2005, pp. 103–106.

[49] N. Cobelli, J. Hardin, and L. Santambrogio, "Mediators of the inflammatory response to joint replacement devices," *Osteoarthr. Cartil.*, vol. 7, pp. 600–608, 2011.

[50] Z. Shen, T. N. Crotti, K. P. McHugh, K. Matsuzaki, E. M. Gravallese, B. E. Bierbaum, and S. R. Goldring, "The role played by cell-substrate interactions in the pathogenesis of osteoclast-mediated peri-implant osteolysis," *Arthritis Res. Ther.*, vol. 8, no. 3, p. R70, 2006.

[51] H. G. Willert, H. Bertram, and G. H. Buchhorn, "Osteolysis in alloarthroplasty of the hip. The role of ultra-high molecular weight polyethylene wear particles," *Clin. Orthop. Relat. Res.*, vol. 258, pp. 95–107, 1990.

[52] R. A. Cooper, C. M. McAllister, L. S. Borden, and T. W. Bauer, "Polyethylene debris-induced osteolysis and loosening in uncemented total hip arthroplasty. A cause of late failure," *J. Arthroplasty*, vol. 7, no. 3, pp. 285–290, 1992.

[53] H. C. Amstutz, P. Campbell, N. Kossovsky, and I. C. Clarke, "Mechanism and clinical significance of wear debris-induced osteolysis," *Clin. Orthop. Relat. Res.*, vol. 276, pp. 7–18, 1992.

[54] A. G. Cobb and T. P. Schmalzreid, "The clinical significance of metal ion release from cobalt-chromium metal-on-metal hip joint arthroplasty," *Proc. Inst. Mech. Eng. H.*, vol. 220, no. 2, pp. 385–398, 2006.

[55] P. F. Doorn, P. A. Campbell, J. Worrall, P. D. Benya, H. A. McKellop, and H. C. Amstutz, "Metal wear particle characterization from metal on metal total hip replacements: transmission electron microscopy study of periprosthetic tissues and isolated particles," *J. Biomed. Mater. Res.*, vol. 42, no. 1, pp. 103–11, 1998.

[56] E. Ingham and J. Fisher, "Biological reactions to wear debris in total joint replacement," *Proc. Inst. Mech. Eng. H.*, vol. 214, no. 1, pp. 21–37, 2000.

[57] H. Baudriller, P. Chabrand, and D. Moukoko, "Modeling UHMWPE wear debris generation," *J. Biomed. Mater. Res. B. Appl. Biomater.*, vol. 80, no. 2, pp. 479–85, 2007.

[58] P. Campbell, S. Ma, B. Yeom, H. McKellop, T. P. Schmalzried, and H. C. Amstutz, "Isolation of predominantly submicron-sized UHMWPE wear particles from periprosthetic tissues," *J. Biomed. Mater. Res. A.*, vol. 29, no. 1, pp. 127–131, 1995.

[59] M. Visentin, S. Stea, S. Squarzoni, B. Antonietti, M. Reggiani, and A. Toni, "A new method for isolation of polyethylene wear debris from tissue and synovial fluid," *Biomaterials*, vol. 25, no. 24, pp. 5531–7, 2004.

[60] T. R. Yoon, S. M. Rowe, S. T. Jung, K. J. Seon, and W. J. Maloney, "Osteolysis in association with a total hip arthroplasty with ceramic bearing surfaces," *J. Bone Joint Surg. Am.*, vol. 80, no. 10, pp. 1459–68, 1998.

[61] J. L. Tipper, P. J. Firkins, A. A. Besong, P. S. M. Barbour, J. Nevelos, M. H. Stone, E. Ingham, and J. Fisher, "Characterisation of wear debris from UHMWPE on zirconia ceramic, metal-on-metal and alumina ceramic-on-ceramic hip prostheses generated in a physiological anatomical hip joint simulator," *Wear*, vol. 250, no. 2, pp. 120–128, 2001.

[62] A. Hatton, J. E. Nevelos, A. A. Nevelos, R. E. Banks, J. Fisher, and E. Ingham, "Alumina-alumina artificial hip joints. Part I: A histological analysis and characterisation of wear debris by laser capture microdissection of tissues retrieved at revision," *Biomaterials*, vol. 23, no. 16, pp. 3429–3440, 2002.

[63] I. Catelas, P. A. Campbell, J. D. Bobyn, J. B. Medley, and O. L. Huk, "Wear particles from metal-on-metal total hip replacements: effects of implant design and implantation time," *Proc. Inst. Mech. Eng. H.*, vol. 220, no. 2, pp. 195–208, 2006.

[64] R. J. Looney, E. M. Schwarz, A. Boyd, and R. J. O'Keefe, "Periprosthetic osteolysis: an immunologist's update," *Curr. Opin. Rheumatol.*, vol. 18, no. 1, pp. 80–7, 2006.

[65] A. Sargeant and T. Goswami, "Pathophysiological aspects of hip implants," *J. Surg. Orthop. Adv.*, vol. 15, no. 2, pp. 111–112, 2006.

[66] P. E. Purdue, P. Koulouvaris, H. G. Potter, B. J. Nestor, and T. P. Sculco, "The cellular and molecular biology of periprosthetic osteolysis," *Clin. Orthop. Relat. Res.*, vol. 454, pp. 251–261, 2007.

[67] T. A. Blaine, R. N. Rosier, J. E. Puzas, R. J. Looney, P. R. Reynolds, S. D. Reynolds, and R. J. O'Keefe, "Increased levels of tumor necrosis factor-alpha and interleukin-6 protein and messenger RNA in human peripheral blood monocytes due to titanium particles," *J. Bone Joint Surg. Am.*, vol. 78, no. 8, pp. 1181–1192, 1996.

[68] S. V. Bukata, J. Gelinas, X. Wei, R. N. Rosier, J. E. Puzas, X. Zhang, E. M. Schwarz, X. R. Song, D. E. Griswold, and R. J. O'Keefe, "PGE2 and IL-6 production by fibroblasts in response to titanium wear debris particles is mediated through a Cox-2 dependent pathway," *J. Orthop. Res.*, vol. 22, no. 1, pp. 6–12, 2004.

[69] S. Goodman, "Wear particulate and osteolysis," *Orthop. Clin. North Am.*, vol. 36, no. 1, pp. 41–48, 2005.

[70] R. Maitra, C. C. Clement, B. Scharf, G. M. Crisi, S. Chitta, D. Paget, P. E. Purdue, N. Cobelli, and L. Santambrogio, "Endosomal damage and TLR2 mediated inflammasome activation by alkane particles in the generation of aseptic osteolysis," *Mol. Immunol.*, vol. 47, no. 2–3, pp. 175–184, 2009.

[71] P. Campbell and M. Wang, "Positive cytokine production in failed metal-on-metal total hip replacements," *Acta Orthop. Scand.*, vol. 73, no. 5, pp. 506–512, 2002.

[72] I. Catelas, P. A. Campbell, F. Dorey, A. Frausto, B. G. Mills, and H. C. Amstutz, "Semi-quantitative analysis of cytokines in MM THR tissues and their relationship to metal particles," *Biomaterials*, vol. 24, no. 26, pp. 4785–4797, 2003.

[73] J. Gallo, J. Vaculova, S. B. Goodman, Y. T. Konttinen, and J. P. Thyssen, "Contributions of human tissue analysis to understanding the mechanisms of loosening and osteolysis in total hip replacement," *Acta Biomater.*, vol. 10, no. 6, pp. 2354–2366, 2014.

[74] D. R. Haynes, T. N. Crotti, a E. Potter, M. Loric, G. J. Atkins, D. W. Howie, and D. M. Findlay, "The osteoclastogenic molecules RANKL and RANK are associated with periprosthetic osteolysis," *J. Bone Joint Surg. Br.*, vol. 83, no. 6, pp. 902–911, 2001.

[75] C.-T. Wang, Y.-T. Lin, B.-L. Chiang, S.-S. Lee, and S.-M. Hou, "Over-expression of receptor activator of nuclear factor-kappaB ligand (RANKL), inflammatory cytokines, and chemokines in periprosthetic osteolysis of loosened total hip arthroplasty," *Biomaterials*, vol. 31, no. 1, pp. 77–82, 2010.

[76] R. A. Smith, A. Maghsoodpour, and N. J. Hallab, "In vivo response to cross-linked polyethylene and polycarbonate-urethane particles," *J. Biomed. Mater. Res. A.*, vol. 93, no. 1, pp. 227–234, 2010.

[77] B. F. Boyce, E. M. Schwarz, and L. Xing, "Osteoclast precursors: cytokine-stimulated immunomodulators of inflammatory bone disease," *Curr. Opin. Rheumatol.*, vol. 18, no. 4, pp. 427–32, 2006.

[78] Y. Wu, M. B. Humphrey, and M. C. Nakamura, "Osteoclasts - the innate immune cells of the bone," *Autoimmunity*, vol. 41, no. 3, pp. 183–194, 2008.

[79] M. Alnaeeli and Y. A. Teng, "Dendritic cells differentiate into osteoclasts in bone marrow microenvironment in vivo," *Blood*, vol. 113, no. 1, pp. 264–265, 2009.

[80] R. Lenz, W. Mittelmeier, D. Hansmann, R. Brem, P. Diehl, A. Fritsche, and R. Bader, "Response of human osteoblasts exposed to wear particles generated at the interface of total hip stems and bone cement," *J. Biomed. Mater. Res. A.*, vol. 89, no. 2, pp. 370–378, 2008.

[81] M. L. Wang, L. J. Nesti, R. Tuli, J. Lazatin, K. G. Danielson, P. F. Sharkey, and R. S. Tuan, "Titanium particles suppress expression of osteoblastic phenotype in human mesenchymal stem cells," *J. Orthop. Res.*, vol. 20, no. 6, pp. 1175–1184, 2002.

[82] C. Vermes, R. Chandrasekaran, J. J. Jacobs, J. O. Galante, K. a Roebuck, and T. T. Glant, "The effects of particulate wear debris, cytokines, and growth factors on the functions of MG-63 osteoblasts," *J. Bone Joint Surg. Am.*, vol. 83, no. 2, pp. 201–211, 2001.

[83] D. P. Pioletti, L. Leoni, D. Genini, H. Takei, P. Du, and J. Corbeil, "Gene expression analysis of osteoblastic cells contacted by orthopedic implant particles," *J. Biomed. Mater. Res.*, vol. 61, no. 3, pp. 408–420, 2002.

[84] I. Catelas, A. Petit, D. J. Zukor, J. Antoniou, and O. L. Huk, "TNF-alpha secretion and macrophage mortality induced by cobalt and chromium ions in vitro - Qualitative analysis of apoptosis," *Biomaterials*, vol. 24, no. 3, pp. 383–391, 2003.

[85] J. Yang and J. Black, “Competitive binding of chromium, cobalt and nickel to serum proteins,” *Biomaterials*, vol. 15, no. 4, pp. 262–268, 1994.

[86] N. J. Hallab, M. Caicedo, R. Epstein, K. McAllister, and J. J. Jacobs, “In vitro reactivity to implant metals demonstrates a person dependent association with both T-cell and B-cell activation,” *J. Biomed. Mater. Res. A.*, vol. 92, no. 2, pp. 667–682, 2010.

[87] G. Iolascon, G. Di Pietro, A. Capaldo, C. Gioia, S. Gatto, and F. Gimigliano, “Periprosthetic bone density as outcome of therapeutic response,” *Clin. Cases Miner. Bone Metab.*, vol. 7, no. 1, pp. 27–31, 2010.

[88] P. J. Mease, B. S. Goffe, J. Metz, A. VanderStoep, B. Finck, and D. J. Burge, “Etanercept in the treatment of psoriatic arthritis and psoriasis: a randomised trial,” *Lancet*, vol. 356, no. 9227, pp. 385–90, 2000.

[89] L. M. Childs, J. J. Goater, R. J. O’Keefe, and E. M. Schwarz, “Efficacy of etanercept for wear debris-induced osteolysis,” *J. bone Miner. Res.*, vol. 16, no. 2, pp. 338–347, 2001.

[90] E. M. Schwarz, R. J. O’Keefe, D. Campbell, S. Totterman, A. Boyd, and R. J. Looney, “Use of volumetric computerized tomography as a primary outcome measure to evaluate drug efficacy in the prevention of peri-prosthetic osteolysis: a 1-year clinical pilot of etanercept vs. placebo,” *J. Orthop. Res.*, vol. 21, no. 6, pp. 1049–55, 2003.

[91] J. S. Sun, F. H. Lin, Y. H. Tsuang, L. T. Chen, R. C. Hong, W. H. S. Chang, and H. C. Liu, “Effect of anti-inflammatory medication on monocyte response to titanium particles,” *J. Biomed. Mater. Res.*, vol. 52, no. 3, pp. 509–516, 2000.

[92] P. F. Pollice, R. N. Rosier, R. J. Looney, J. E. Puzas, S. E. M, and Regis J.O’Keefe, “Oral pentoxifylline inhibits release of tumor necrosis factor-alpha from human peripheral blood monocytes,” *J. Bone Joint Surg. Am.*, vol. 83, no. 7, pp. 1057–1061, 2001.

[93] “Safety Update on TNF-α Antagonists: Infliximab and Etanercept.” [Online]. Available: http://www.fda.gov/ohrms/dockets/ac/01/briefing/3779b2_01_cber_safety _revision2.pdf.

[94] “Benefits vs risks: What to know about the side effects of ENBREL.” [Online]. Available: https://www.enbrel.com/support/side-effects-safety-information/. [Accessed: 22-Nov-2015].

[95] M. C. Trindade, M. Lind, Y. Nakashima, D. Sun, S. B. Goodman, D. J. Schurman, and R. L. Smith, "Interleukin-10 inhibits polymethylmethacrylate particle induced interleukin-6 and tumor necrosis factor-α release by human monocyte/macrophages in vitro," *Biomaterials*, vol. 22, no. 15, pp. 2067–2073, 2001.

[96] G.-I. Im and J. D. Han, "Suppressive effects of interleukin-4 and interleukin-10 on the production of proinflammatory cytokines induced by titanium-alloy particles," *J. Biomed. Mater. Res.*, vol. 58, no. 5, pp. 531–536, 2001.

[97] D. Clemett and K. L. Goa, "Celecoxib: a review of its use in osteoarthritis, rheumatoid arthritis and acute pain," *Drugs*, vol. 59, no. 4, pp. 957–980, 2000.

[98] X. Zhang, S. G. Morham, R. Langenbach, D. A. Young, L. Xing, B. F. Boyce, J. E. Puzas, R. N. Rosier, R. J. O'Keefe, and E. M. Schwarz, "Evidence for a direct role of cyclo-oxygenase 2 in implant wear debris-induced osteolysis," *J. Bone Miner. Res.*, vol. 16, no. 4, pp. 660–670, 2001.

[99] G.-I. Im, B.-C. Kwon, and K.-B. Lee, "The effect of COX-2 inhibitors on periprosthetic osteolysis," *Biomaterials*, vol. 25, no. 2, pp. 269–275, 2004.

[100] E. M. Schwarz, "What potential biologic treatments are available for osteolysis?," *J. Am. Acad. Orthop. Surg.*, vol. 16, no. 1, pp. S72–5, 2008.

[101] P. Gazzerro, M. C. Proto, G. Gangemi, A. M. Malfitano, E. Ciaglia, S. Pisanti, A. Santoro, C. Laezza, and M. Bifulco, "Pharmacological actions of statins: a critical appraisal in the management of cancer," *Pharmacol. Rev.*, vol. 64, no. 1, pp. 102–46, 2012.

[102] S. Bellosta, R. Paoletti, and A. Corsini, "Safety of statins: focus on clinical pharmacokinetics and drug interactions," *Circulation*, vol. 109, no. 23, pp. 50–57, 2004.

[103] S. Elavarasu, T. K. Suthanthiran, and D. Naveen, "Statins: A new era in local drug delivery," *J. Pharm. Bioallied Sci.*, vol. 4, no. 2, pp. 248–51, 2012.

[104] C. Stancu and A. Sima, "Statins: mechanism of action and effects," *J. Cell. Mol. Med.*, vol. 5, no. 4, pp. 378–387, 2001.

[105] A. Lübbeke, G. Garavaglia, K. J. Rothman, A. Bonvin, C. Roussos, H. Miozzari, and P. Hoffmeyer, "Statins may reduce femoral osteolysis in patients with total Hip arthroplasty," *J. Orthop. Res.*, vol. 31, no. 5, pp. 814–20, 2013.

[106] T. M. Thillemann, “The risk of revision after primary total hip arthroplasty among statin users: A nationwide population-based nested case-control study,” *J. Bone Joint Surg.*, vol. 92, no. 5, pp. 1063–1072, 2010.

[107] M. K. Yildiz, I. Okan, N. Dursun, G. Bas, O. Alimoglu, B. Kaya, and M. Sahin, “Effect of orally administered simvastatin on prevention of postoperative adhesion in rats,” *Int. J. Clin. Exp. Med.*, vol. 7, no. 2, pp. 405–10, 2014.

[108] F. Ungaro, C. Giovino, O. Catanzano, A. Miro, A. Mele, F. Quaglia, and M. I. La Rotonda, “Use of cyclodextrins as solubilizing agents for simvastatin: Effect of hydroxypropyl-beta-cyclodextrin on lactone/hydroxyacid aqueous equilibrium,” *Int. J. Pharm.*, vol. 404, no. 1–2, pp. 49–56, 2011.

[109] “Simvastatin Structural Formulae.” [Online]. Available: https://commons.wikimedia.org/wiki/File:Simvastatin_Structural_Formulae.png. [Accessed: 23-Nov-2015].

[110] B. P. Leung, N. Sattar, A. Crilly, M. Prach, D. W. McCarey, H. Payne, and I. B. McInnes, “A novel anti-inflammatory role for simvastatin in inflammatory arthritis,” *J. Immunol.*, vol. 170, no. 3, pp. 1524–1530, 2003.

[111] M. Djaldetti, H. Salman, M. Bergman, and H. Bessler, “Effect of pravastatin, simvastatin and atorvastatin on the phagocytic activity of mouse peritoneal macrophages,” *Exp. Mol. Pathol.*, vol. 80, no. 2, pp. 160–164, 2006.

[112] L. Diomede, D. Albani, M. Sottocorno, M. B. Donati, M. Bianchi, P. Fruscella, and M. Salmona, “In vivo anti-inflammatory effect of statins is mediated by nonsterol mevalonate products,” *Arterioscler. Thromb. Vasc. Biol.*, vol. 21, no. 8, pp. 1327–1332, 2001.

[113] T. J. Stalker, A. M. Lefer, and R. Scalia, “A new HMG-CoA reductase inhibitor, rosuvastatin, exerts anti-inflammatory effects on the microvascular endothelium: the role of mevalonic acid,” *Br. J. Pharmacol.*, vol. 133, no. 3, pp. 406–412, 2001.

[114] M. Kimura, I. Kurose, J. Russell, and D. N. Granger, “Effects of fluvastatin on leukocyte-endothelial cell adhesion in hypercholesterolemic rats,” *Arterioscler. Thromb. Vasc. Biol.*, vol. 17, pp. 1521–1526, 1997.

[115] Y. Takuwa, C. Ohse, E. A. Wang, J. M. Wozney, and K. Yamashita, "Bone morphogenetic protein-2 stimulates alkaline phosphatase activity and collagen synthesis in cultured osteoblastic cells, MC3T3-E1," *Biochem. Biophys. Res. Commun.*, vol. 174, no. 1, pp. 96–101, 1991.

[116] T. Maeda, A. Matsunuma, I. Kurahashi, T. Yanagawa, H. Yoshida, and N. Horiuchi, "Induction of osteoblast differentiation indices by statins in MC3T3-E1 cells," *J. Cell. Biochem.*, vol. 92, pp. 458–471, 2004.

[117] Y. Zhou, Y. Ni, Y. Liu, B. Zeng, Y. Xu, and W. Ge, "The role of simvastatin in the osteogenesis of injectable tissue-engineered bone based on human adipose-derived stromal cells and platelet-rich plasma," *Biomaterials*, vol. 31, no. 20, pp. 5325–35, 2010.

[118] P. Verma, A. S. Thakur, K. Deshukh, A. K. Jha, and S. Verma, "Routes of drug administration," *Int. J. Pharm. Stud. Res.*, vol. 1, no. 1, pp. 54–59, 2010.

[119] L. Rejnmark, N. H. Buus, P. Vestergaard, L. Heickendorff, F. Andreasen, M. L. Larsen, and L. Mosekilde, "Effects of simvastatin on bone turnover and BMD: a 1-year randomized controlled trial in postmenopausal osteopenic women," *J. Bone Miner. Res.*, vol. 19, no. 5, pp. 737–44, 2004.

[120] J. A. de Lemos, M. A. Blazing, S. D. Wiviott, E. F. Lewis, K. A. Fox, H. D. White, J.-L. Rouleau, T. R. Pedersen, L. H. Gardner, R. Mukherjee, K. E. Ramsey, J. Palmisano, D. W. Bilheimer, M. A. Pfeffer, R. M. Califf, and E. Braunwald, "Early intensive vs a delayed conservative simvastatin strategy in patients with acute coronary syndromes: phase Z of the A to Z trial," *J. Am. Med. Assoc.*, vol. 292, no. 11, pp. 1307–1316, 2004.

[121] J. Hippisley-Cox and C. Coupland, "Individualising the risks of statins in men and women in England and Wales: population-based cohort study," *Br. Med. J.*, vol. 96, no. 12, pp. 939–947, 2010.

[122] R. G. Fassett and J. S. Coombes, "Use of high potency statins and rates of admission for acute kidney injury: multicenter, retrospective observational analysis of administrative databases," *Br. Med. J.*, vol. 346, p. DOI:[10.1136/bmj.f1531], 2013.

[123] H. Vaziri, R. Naserhojjati-Roodsari, N. Tahsili-Fahadan, A. Khojasteh, F. Mashhadi-Abbas, B. Eslami, and A. R. Dehpour, "Effect of simvastatin administration on periodontitis-associated bone loss in ovariectomized rats," *J. Periodontol.*, vol. 78, no. 8, pp. 1561–7, 2007.

[124] M. S. Morris, Y. Lee, M. T. Lavin, P. J. Giannini, M. J. Schmid, D. B. Marx, and R. A. Reinhardt, "Injectable simvastatin in periodontal defects and alveolar ridges: pilot studies," *J. Periodontol.*, vol. 79, no. 8, pp. 1465–73, 2008.

[125] N. Yang, Y. Cui, J. Tan, X. Fu, X. Han, H. Leng, and C. Song, "Local injection of a single dose of simvastatin augments osteoporotic bone mass in ovariectomized rats," *J. Bone Miner. Metab.*, vol. 32, no. 3, pp. 252–60, 2014.

[126] M. Thylin and J. McConnell, "Effects of simvastatin gels on murine calvarial bone," *J. Periodontol.*, vol. 73, pp. 1141–1148, 2002.

[127] D. Stein, Y. Lee, M. J. Schmid, B. Killpack, M. a Genrich, N. Narayana, D. B. Marx, D. M. Cullen, and R. a Reinhardt, "Local simvastatin effects on mandibular bone growth and inflammation," *J. Periodontol.*, vol. 76, no. 11, pp. 1861–1870, 2005.

[128] M. Nyan, D. Sato, M. Oda, T. Machida, H. Kobayashi, T. Nakamura, and S. Kasugai, "Bone formation with the combination of simvastatin and calcium sulfate in critical-sized rat calvarial defect," *J. Pharmacol. Sci.*, vol. 104, pp. 384–386, 2007.

[129] M. N. Ravi Kumar, "Nano and microparticles as controlled drug delivery devices," *J. Pharm. Pharm. Sci.*, vol. 3, no. 2, pp. 234–58, 2000.

[130] I.-C. Tai, Y.-C. Fu, C.-K. Wang, J.-K. Chang, and M.-L. Ho, "Local delivery of controlled-release simvastatin/PLGA/HAp microspheres enhances bone repair," *Int. J. Nanomedicine*, vol. 8, pp. 3895–904, 2013.

[131] B. Sarmento, A. J. Ribeiro, F. Veiga, D. C. Ferreira, and R. J. Neufeld, "Insulin-loaded nanoparticles are prepared by alginate ionotropic pre-gelation followed by chitosan polyelectrolyte complexation," *J. Nanosci. Nanotechnol.*, vol. 7, no. 8, pp. 2833–2841, 2007.

[132] H. K. Makadia and S. J. Siegel, "Poly Lactic-co-Glycolic Acid (PLGA) as biodegradable controlled drug delivery carrier," *Polymers*, vol. 3, no. 3, pp. 1377–1397, 2011.

[133] A. Shilpa, S. S. Agrawal, and A. R. Ray, "Controlled delivery of drugs from alginate matrix," *J. Macromol. Sci. Polym. Rev.*, vol. 43, no. 2, pp. 187–221, 2003.

[134] T. Jiang, N. Han, B. Zhao, Y. Xie, and S. Wang, "Enhanced dissolution rate and oral bioavailability of simvastatin nanocrystal prepared by sonoprecipitation," *Drug Dev. Ind. Pharm.*, vol. 38, no. 10, pp. 1230–9, 2012.

[135] X. Wang and M. L. Brusseau, “Solubilization of some low-polarity organic compounds by hydroxypropyl- beta-cyclodextrin,” *Environ. Sci. Technol.*, vol. 27, no. 13, pp. 2821–2825, 1993.

[136] S. Gould and R. C. Scott, “2-Hydroxypropyl-β-cyclodextrin (HP-β-CD): A toxicology review,” *Food Chem. Toxicol.*, vol. 43, no. 10, pp. 1451–1459, 2005.

[137] “(2-Hydroxypropyl)-Beta-Cyclodextrin.” [Online]. Available: http://www.chemicalbook.com/ChemicalProductProperty_EN_CB6204503.htm. [Accessed: 23-Nov-2015].

[138] W. Song, F. Wang, P. Lotfi, M. Sardiello, and L. Segatori, “2-hydroxypropyl-β-cyclodextrin promotes TFEB-mediated activation of autophagy: implications for therapy,” *J. Biol. Chem.*, vol. 289, no. 14, pp. 10211–22, 2014.

[139] S. W. Jun, M. Kim, J. Kim, H. Jun, S. Lee, J. Woo, and S. Hwang, “Preparation and characterization of simvastatin / hydroxypropyl-β-cyclodextrin inclusion complex using supercritical antisolvent (SAS) process,” *Eur. J. Pharm. Biopharm.*, vol. 66, no. 3, pp. 413–421, 2007.

[140] S. Shiralashetti, A. Patil, and J. Patil, “Influence of method of preparation on solubility , physicochemical properties and in-vitro release profile of Simvastatin- cyclodextrin inclusion complexes : A comparative study,” *Int. J. ChemTech Res.*, vol. 2, no. 1, pp. 562–571, 2010.

[141] T. A. Premchandani and B. B. Barik, “Preparation and statistical optimization of alginate based stomach specific floating microcapsules of simvastatin,” *Acta Polymer Pharm.*, vol. 69, no. 4, pp. 751–61, 2012.

[142] M. Yoshinari, K. Matsuzaka, S. Hashimoto, K. Ishihara, T. Inoue, Y. Oda, T. Ide, and T. Tanaka, “Controlled release of simvastatin acid using cyclodextrin inclusion system,” *Dent. Mater. J.*, vol. 26, no. 3, pp. 451–456, 2007.

[143] “Alginate.” [Online]. Available: http://www1.lsbu.ac.uk/water/alginate.html. [Accessed: 23-Nov-2015].

[144] J. P. Paques, E. van der Linden, C. J. van Rijn, and L. M. Sagis, “Preparation methods of alginate nanoparticles,” *Adv. Colloid Interface Sci.*, vol. 209, pp. 163–171, 2014.

[145] T. A. Becker, D. R. Kipke, and T. Brandon, “Calcium alginate gel: A biocompatible and mechanically stable polymer for endovascular embolization,” *J. Biomed. Mater. Res.*, vol. 54, no. 1, pp. 76–86, 2001.

[146] G. T. Grant, E. R. Morris, D. a. Rees, P. J. C. Smith, and D. Thom, “Biological interactions between polysaccharides and divalent cations: The egg-box model,” *FEBS Lett.*, vol. 32, no. 1, pp. 195–198, 1973.

[147] J. F. A. Valente, V. M. Gaspar, B. P. Antunes, P. Countinho, and I. J. Correia, “Microencapsulated chitosan–dextran sulfate nanoparticles for controled delivery of bioactive molecules and cells in bone regeneration,” *Polymer*, vol. 54, no. 1, pp. 5–15, 2013.

[148] T. A. Read, V. Stensvaag, H. Vindenes, E. Ulvestad, R. Bjerkvig, and F. Thorsen, “Cells encapsulated in alginate: A potential system for delivery of recombinant proteins to malignant brain tumours,” *Int. J. Dev. Neurosci.*, vol. 17, no. 5, pp. 653–663, 1999.

[149] J. Sun and H. Tan, “Alginate-based biomaterials for regenerative medicine applications,” *Materials*, vol. 6, no. 4, pp. 1285–1309, 2013.

[150] X. Hu and D. L. Kaplan, “Silk biomaterials,” in *Comprehensive biomaterials*, P. Ducheyne, K. Healy, D. E. Hutmacher, D. W. Grainger, and C. J. Kirkpatrick, Eds. Elsevier, 2011, pp. 208–219.

[151] R. K. Das, N. Kasoju, and U. Bora, “Encapsulation of curcumin in alginate-chitosan-pluronic composite nanoparticles for delivery to cancer cells,” *Nanomed. Nanotech. Biol. Med.*, vol. 6, no. 1, pp. 153–60, 2010.

[152] F. Wang, Y. Chen, D. Zhang, Q. Zhang, D. Zheng, L. Hao, Y. Liu, C. Duan, L. Jia, and G. Liu, “Folate-mediated targeted and intracellular delivery of paclitaxel using a novel deoxycholic acid-O-carboxymethylated chitosan-folic acid micelles,” *Int. J. Nanomedicine*, vol. 7, pp. 325–337, 2012.

[153] H. Guo, Q. Lai, W. Wang, Y. Wu, C. Zhang, Y. Liu, and Z. Yuan, “Functional alginate nanoparticles for efficient intracellular release of doxorubicin and hepatoma carcinoma cell targeting therapy,” *Int. J. Pharm.*, vol. 451, no. 1–2, pp. 1–11, 2013.

[154] S. Bhunchu and P. Rojsitthisak, “Biopolymeric alginate-chitosan nanoparticles as drug delivery carriers for cancer therapy,” *Die Pharm.*, vol. 69, no. 8, pp. 563–570, 2014.

[155] X. Wang, L. Yang, Z. G. Chen, and D. M. Shin, "Application of nanotechnology in cancer therapy and imaging," *CA. Cancer J. Clin.*, vol. 58, no. 2, pp. 97–110, 2008.

[156] T. Alexakis, D. K. Boadi, D. Quong, A. Groboillot, I. O'Neill, D. Poncelet, R. J. Neufeld, I. Neill, D. Poncelet, and R. J. Neufeld, "Microencapsulation of DNA within alginate microspheres and crosslinked chitosan membranes for in vivo application," *Appl. Biochem. Biotechnol.*, vol. 50, no. 1, pp. 93–106, 1995.

[157] D. Quong and R. J. Neufeld, "DNA protection from extracapsular nucleases, within chitosan- or poly- L-lysine-coated alginate beads," *Biotechnol. Bioeng.*, vol. 60, no. 1, pp. 124–134, 1998.

[158] R. J. Mumper, A. S. Huffman, P. A. Puolakkainen, L. S. Bouchard, and W. R. Gombotz, "Calcium-alginate beads for the oral delivery of transforming growth factor-β1 (TGF-β1): stabilization of TGF-β1 by the addition of polyacrylic acid within acid-treated beads," *J. Control. Release*, vol. 30, no. 3, pp. 241–251, 1994.

[159] L. Liu, S. Liu, S. Y. Ng, M. Froix, T. Ohno, and J. Heller, "Controlled release of interleukin-2 for tumour immunotherapy using alginate/chitosan porous microspheres," *J. Control. Release*, vol. 43, no. 1, pp. 65–74, 1997.

[160] S. A. Timmy, S. P. Victor, C. P. Sharma, and V. Kumari, "Betacyclodextrin complexed insulin loaded alginate microspheres - oral delivery system," *Trends Biomater. Artif. Organs*, vol. 15, no. 2, pp. 48–53, 2001.

[161] S. Önal and F. Zihniğlu, "Encapsulation of insulin in chitosan-coated alginate beads: oral therapeutic peptide delivery," *Artif. Cells. Blood Substit. Immobil. Biotechnol.*, vol. 30, no. 3, pp. 229–237, 2002.

[162] G. Coppi, V. Iannuccelli, E. Leo, M. T. Bernabei, and R. Cameroni, "Protein immobilization in crosslinked alginate microparticles," *J. Microencapsul.*, vol. 19, no. 1, pp. 37–44, 2002.

[163] C. M. Silva, A. J. Ribeiro, M. Figueiredo, D. Ferreira, and F. Veiga, "Microencapsulation of hemoglobin in chitosan-coated alginate microspheres prepared by emulsification/internal gelation," *AAPS J.*, vol. 7, no. 4, pp. E903–E913, 2005.

[164] S. Martins, B. Sarmento, E. B. Souto, and D. C. Ferreira, “Insulin-loaded alginate microspheres for oral delivery - Effect of polysaccharide reinforcement on physicochemical properties and release profile,” *Carbohydr. Polym.*, vol. 69, no. 4, pp. 725–731, 2007.

[165] D. K. Boadi and R. J. Neufeld, “Encapsulation of tannase for the hydrolysis of tea tannins,” *Enzym. Microb. Technol.*, vol. 28, no. 7–8, pp. 590–595, 2001.

[166] A. R. DeGroot and R. J. Neufeld, “Encapsulation of urease in alginate beads and protection from α-chymotrypsin with chitosan membranes,” *Enzym. Microb. Technol.*, vol. 29, no. 6–7, pp. 321–327, 2001.

[167] C. C. Ribeiro, C. C. Barrias, and M. A. Barbosa, “Calcium phosphate-alginate microspheres as enzyme delivery matrices,” *Biomaterials*, vol. 25, no. 18, pp. 4363–4373, 2004.

[168] P. R. Hari, T. Chandy, C. P. Sharma, and C. P. Sharmat, “Chitosan/calcium alginate microcapsules for intestinal delivery of nitrofurantoin,” *J. Microencapsul.*, vol. 13, no. 3, pp. 319–329, 1996.

[169] M. Albarghouthi, D. A. Fara, M. Saleem, T. El-Thaher, K. Matalka, and A. Badwan, “Immobilization of antibodies on alginate-chitosan beads,” *Int. J. Pharm.*, vol. 206, pp. 23–34, 2000.

[170] X. Li, “The use of chitosan to increase the stability of calcium alginate beads with entrapped yeast cells,” *Biochem. Appl. Biochem.*, vol. 23, pp. 269–72, 1996.

[171] Y. Zhou, E. Martins, A. Groboillot, C. Champagne, and R. J. Neufeld, “Spectrophotometric quantification of lactic bacteria in alginate and control of cell release with chitosan coating,” *J. Appl. Microbiol.*, vol. 84, no. 3, pp. 342–348, 1998.

[172] T. Chandy, D. L. Mooradian, and G. H. R. Rao, “Evaluation of modified alginate-chitosan-polyethylene glycol microcapsules for cell encapsulation,” *Artif. Organs*, vol. 23, no. 10, pp. 894–903, 1999.

[173] G. Klinkenberg, K. Q. Lystad, T. D. W. Levine, and N. Dyrset, “Cell release from alginate immobilized Lactococcus lactis ssp. lactis in chitosan and alginate coated beads,” *J. Dairy Sci.*, vol. 84, no. 5, pp. 1118–1127, 2001.

[174] D. A. Lee, T. Reisler, and D. L. Bader, “Expansion of chondrocytes for tissue engineering in alginate beads enhances chondrocytic phenotype compared to conventional monolayer techniques,” *Acta Orthop. Scand.*, vol. 74, no. 1, pp. 6–15, 2003.

[175] M. Grellier, P. L. Granja, J.-C. Fricain, S. J. Bidarra, M. Renard, R. Bareille, C. Bourget, J. Amédée, and M. A. Barbosa, “The effect of the co-immobilization of human osteoprogenitors and endothelial cells within alginate microspheres on mineralization in a bone defect,” *Biomaterials*, vol. 30, no. 19, pp. 3271–3278, 2009.

[176] A. Vyas, Æ. S. Saraf, and Æ. S. Saraf, “Encapsulation of cyclodextrin complexed simvastatin in chitosan nanocarriers : A novel technique for oral delivery,” *J. Incl. Phenom. Macrocycl. Chem.*, vol. 66, no. 3, pp. 251–259, 2010.

[177] N. K. Comolli and C. E. Clark, “Polymeric microparticles,” in *Engineering polymer systems for improved drug delivery*, R. A. Bader and D. A. Putnam, Eds. Hoboken: John Wiley & Sons, Inc., 2014, pp. 85–116.

[178] M. S. Reza, M. A. Quadir, and S. S. Haider, “Comparative evaluation of plastic, hydrophobic and hydrophilic polymers as matrices for controlled-release drug delivery,” *J. Pharm. Pharm. Sci.*, vol. 6, no. 2, pp. 282–291, 2003.

[179] D. Lemoine, F. Wauters, S. Bouchend, and V. Pre, “Preparation and characterization of alginate microspheres containing a model antigen,” *Int. J. Pharm.*, vol. 176, no. 1, pp. 9–19, 1998.

[180] M. K. Das and P. C. Senapati, “Evaluation of furosemide-loaded alginate microspheres prepared by ionotropic external gelation technique,” *Acta Pol. Pharm.*, vol. 64, no. 3, pp. 253–262, 2007.

[181] A. Rajendran and S. K. Basu, “Alginate-chitosan particulate system for sustained release of nimodipine,” *Trop. J. Pharm. Res.*, vol. 8, no. 5, pp. 433–440, 2009.

[182] C. K. Kim and E. J. Lee, “The controlled release of blue dextran from alginate beads,” *Int. J. Pharm.*, vol. 79, no. 1, pp. 11–19, 1992.

[183] J. Ribeiro, C. Silva, D. Ferreira, and F. Veiga, “Chitosan-reinforced alginate microspheres obtained through the emulsification / internal gelation technique,” *Eur. J. Pharm. Sci.*, vol. 25, pp. 31–40, 2005.

[184] I. Andresen, O. Skipnes, and O. S. Ød, “Some biological functions of matrix components in benthic algae in relation to their chemistry and the composition of seawater,” *Cellul. Chem. Technol.*, vol. 6, pp. 361–381, 1977.

[185] J. Wikström, M. Elomaa, H. Syväjärvi, J. Kuokkanen, M. Yliperttula, P. Honkakoski, and A. Urtti, “Alginate-based microencapsulation of retinal pigment epithelial cell line for cell therapy,” *Biomaterials*, vol. 29, no. 7, pp. 869–876, 2008.

[186] S. Shiraishi, T. Imai, and M. Otagiri, “Controlled-release preparation of indomethacin using calcium alginate gel,” *Biol. Pharm. Bull*, vol. 16, no. 11, pp. 1164–1168, 1993.

[187] S. Jaya, T. D. Durance, and R. Wang, “Physical characterization of drug loaded microcapsules and controlled in vitro release study,” *Open Biomater. J.*, vol. 2, no. 1, pp. 9–17, 2010.

[188] C. Alvarez-Lorenzo, B. Blanco-Fernandez, A. M. Puga, and A. Concheiro, “Crosslinked ionic polysaccharides for stimuli-sensitive drug delivery,” *Adv. Drug Deliv. Rev.*, vol. 65, no. 9, pp. 1148–1171, 2013.

[189] A. H. El-Kamel, O. M. N. Al-Gohary, and E. A. Hosny, “Alginate-diltiazem hydrochloride beads: optimization of formulation factors, in vitro and in vivo availability,” *J. Microencapsul.*, vol. 20, no. 2, pp. 211–225, 2003.

[190] M. Ramadas, W. Paul, K. J. Dileep, Y. Anitha, and C. P. Sharma, “Lipoinsulin encapsulated alginate-chitosan capsules,” *J. Microencapsul.*, vol. 17, no. 4, pp. 405–411, 2000.

[191] T. J. Aspden, J. D. Mason, N. S. Jones, J. Lowe, O. Skaugrud, and L. Illum, “Chitosan as a nasal delivery system: the effect of chitosan solutions on in vitro and in vivo mucociliary transport rates in human turbinates and volunteers,” *J. Pharm. Sci.*, vol. 86, no. 4, pp. 509–13, 1997.

[192] A. J. Ribeiro, R. J. Neufeld, P. Arnaud, and J. C. Chaumeil, “Microencapsulation of lipophilic drugs in chitosan-coated alginate microspheres,” *Int. J. Pharm.*, vol. 187, pp. 115–123, 1999.

[193] W. Krasaekoopt, B. Bhandari, and H. C. Deeth, “Survival of probiotics encapsulated in chitosan-coated alginate beads in yoghurt from UHT- and conventionally treated milk during storage,” *LWT - Food Sci. Technol.*, vol. 39, no. 2, pp. 177–183, 2006.

[194] M. T. Cook, G. Tzortzis, D. Charalampopoulos, and V. V. Khutoryanskiy, “Production and evaluation of dry alginate-chitosan microcapsules as an enteric delivery vehicle for probiotic bacteria,” *Biomacromolecules*, vol. 12, no. 7, pp. 2834–2840, 2011.

[195] S. Takka and A. Gürel, “Evaluation of chitosan/alginate beads using experimental design: formulation and in vitro characterization,” *AAPS Pharm. Sci. Tech.*, vol. 11, no. 1, pp. 460–466, 2010.

[196] A. D. Sezer and J. Akbuga, “Release characteristics of chitosan treated alginate beads: II. Sustained release of a low molecular drug from chitosan treated alginate beads,” *J. Microencapsul.*, vol. 16, no. 6, pp. 687–696, 1999.

[197] K. W. Walton, “The biological behaviour of a new synthetic anticoagulant (dextran sulphate) possessing heparin-like properties,” *Br. J. Pharmacol. Chemother.*, vol. 7, no. 3, pp. 370–391, 1952.

[198] Y. Misirli, E. Oztürk, H. Kurşaklioğlu, and E. B. Denkbaş, “Preparation and characterization of Mitomycin-C loaded chitosan-coated alginate microspheres for chemoembolization,” *J. Microencapsul.*, vol. 22, pp. 167–178, 2005.

[199] J. Shi, N. M. Alves, and J. F. Mano, “Chitosan coated alginate beads containing poly(N-isopropylacrylamide) for dual-stimuli-responsive drug release,” *J. Biomed. Mater. Res. B. Appl. Biomater.*, vol. 84, no. 2, pp. 595–603, 2008.

[200] L. Zhao and Z. Zhang, “Mechanical characterization of biocompatible microspheres and microcapsules by direct compression,” *Artif. Cells Blood Substit. Immobil. Biotechnol.*, vol. 32, no. 1, pp. 25–40, 2004.

[201] M. M. Sadeghi, M. Collinge, R. Pardi, and J. R. Bender, “Simvastatin modulates cytokine-mediated endothelial cell adhesion molecule induction: involvement of an inhibitory G protein,” *J. Immunol.*, vol. 165, pp. 2712–2718, 2000.

[202] J. Venkatesan, I. Bhatnagar, P. Manivasagan, K.-H. Kang, and S.-K. Kim, “Alginate composites for bone tissue engineering: A review,” *Int. J. Biol. Macromol.*, vol. 72, pp. 269–281, 2015.

[203] A. K. Anal, D. Bhopatkar, S. Tokura, H. Tamura, and W. F. Stevens, “Chitosan-alginate multilayer beads for gastric passage and controlled intestinal release of protein,” *Drug Dev. Ind. Pharm.*, vol. 29, no. 6, pp. 713–24, 2003.

[204] A. K. Anal and W. F. Stevens, “Chitosan-alginate multilayer beads for controlled release of ampicillin,” *Int. J. Pharm.*, vol. 290, no. 1–2, pp. 45–54, 2005.

[205] Y. Yeo and K. Park, “Control of encapsulation efficiency and initial burst in polymeric microparticle systems,” *Arch. Pharm. Res.*, vol. 27, no. 1, pp. 1–12, 2004.

[206] Y. L. Patel, P. Sher, and A. P. Pawar, “The effect of drug concentration and curing time on processing and properties of calcium alginate beads containing metronidazole by response surface methodology,” *AAPS Pharm. Sci. Tech.*, vol. 7, no. 4, p. 86, 2006.

[207] A. Abdelbary, N. A. El-gendy, and A. Hosny, “Microencapsulation approach for orally extended delivery of glipizide: in vitro and in vivo evaluation,” *Indian J. Pharm. Sci.*, vol. 74, no. 4, pp. 319–330, 2012.

[208] H. Wong and T. M. Chang, “The microencapsulation of cells within alginate poly-L-lysine microcapsules prepared with the standard single step drop technique: histologically identified membrane imperfections and the associated graft rejection,” *Biomater. Artif. cells, Immobil. Biotechnol.*, vol. 19, no. 4, pp. 675–86, 1991.

[209] T. Kokubo and H. Takadama, “How useful is SBF in predicting in vivo bone bioactivity?,” *Biomaterials*, vol. 27, no. 15, pp. 2907–2915, 2006.

[210] O. Sandoval-Castilla, C. Lobato-Calleros, H. S. García-Galindo, J. Alvarez-Ramírez, and E. J. Vernon-Carter, “Textural properties of alginate-pectin beads and survivability of entrapped Lb. casei in simulated gastrointestinal conditions and in yoghurt,” *Food Res. Int.*, vol. 43, no. 1, pp. 111–117, 2010.

[211] W. P. Voo, P. Ravindra, B. T. Tey, and E. S. Chan, “Comparison of alginate and pectin based beads for production of poultry probiotic cells,” *J. Biosci. Bioeng.*, vol. 111, no. 3, pp. 294–299, 2011.

[212] M. Gaikwad, V. S. Belgamwar, A. Tekade, S. Gattani, and S. Surana, “Formulation and evaluation of floating, pulsatile, multiparticulates using pH-dependent swellable polymers,” *Pharm. Dev. Technol.*, vol. 15, no. 2, pp. 209–16, 2009.

[213] A. Mujtaba, A. Mushir, and K. Kanchan, “Influence of formulation variables and process parameters on the release performance of cefpodoxime proxetil from hydroxypropyl methylcellulose and hydroxypropyl methylcellulose-alginate based matrices,” *Adv. Sci. Eng. Med.*, vol. 5, no. 9, pp. 950–956, 2013.

[214] S. Juste, M. Lessard, N. Henley, M. Ménard, and J. P. Hallé, "Effect of poly-L-lysine coating on macrophage activation by alginate-based microcapsules: Assessment using a new in vitro method," *J. Biomed. Mater. Res. A.*, vol. 72, pp. 389–398, 2005.

[215] S. Darquy, M. E. Pueyo, F. Capron, and G. Reach, "Complement activation by alginate-polylysine microcapsules used for islet transplantation," *Artif. Organs*, vol. 18, no. 12, pp. 898–903, 1994.

[216] A. Renken and D. Hunkeler, "Polyvinylamine-based capsules: a mechanistic study of the formation using alginate and cellulose sulphate," *J. Microencapsul.*, vol. 24, no. 4, pp. 323–36, 2007.

[217] F. Wang, J. Shaw, C. Wu, and Y. Wang, "Microencapsulation with poly (vinyl amine) and alginate," *Biotechnol. Tech.*, vol. 6, no. 2, pp. 185–188, 1992.

[218] B. B. Mandal and S. C. Kundu, "Calcium alginate beads embedded in silk fibroin as 3D dual drug releasing scaffolds," *Biomaterials*, vol. 30, no. 28, pp. 5170–7, 2009.

[219] J. E. Samorezov, C. M. Morlock, and E. Alsberg, "Dual ionic and photo-crosslinked alginate hydrogels for micropatterned spatial control of material properties and cell behavior," *Bioconjug. Chem.*, vol. 26, no. 7, pp. 1339–1347, 2015.

[220] A. B. Jindal, M. N. Wasnik, and H. A. Nair, "Synthesis of thiolated alginate and evaluation of mucoadhesiveness, cytotoxicity and release retardant properties," *Indian J. Pharm. Sci.*, vol. 72, no. 6, pp. 766–74, 2010.

[221] R. Mahou, F. Borcard, V. Crivelli, E. Montanari, S. Passemard, F. Noverraz, S. Gerber-Lemaire, L. Buhler, and C. Wandrey, "Tuning the Properties of Hydrogel Microspheres by Adding Chemical Cross-linking Functionality to Sodium Alginate," *Chem. Mater.*, vol. 27, pp. 4380–4389, 2015.

[222] M. Arslan, T. N. Gevrek, A. Sanyal, and R. Sanyal, "Cyclodextrin mediated polymer coupling via thiol–maleimide conjugation: facile access to functionalizable hydrogels," *RSC Adv.*, vol. 4, no. 101, pp. 57834–57841, 2014.

[223] W. L. Stoppel, J. C. White, S. D. Horava, A. C. Henry, S. C. Roberts, and S. R. Bhatia, "Terminal sterilization of alginate hydrogels: Efficacy and impact on mechanical properties," *J. Biomed. Mater. Res. B. Appl. Biomater.*, vol. 102, no. 4, pp. 877–884, 2013.

[224] M. Xu, E. R. West-Farrell, R. L. Stouffer, L. D. Shea, T. K. Woodruff, and M. B. Zelinski, "Encapsulated three-dimensional culture supports development of nonhuman primate secondary follicles," *Biol. Reprod.*, vol. 81, no. 3, pp. 587–94, 2009.

[225] A. Bhat, A. I. Hoch, M. L. Decaris, and J. K. Leach, "Alginate hydrogels containing cell-interactive beads for bone formation," *FASEB J.*, vol. 27, no. 12, pp. 4844–4852, 2013.

[226] E. M. Chandler, C. M. Berglund, J. S. Lee, W. J. Polacheck, J. P. Gleghorn, B. J. Kirby, and C. Fischbach, "Stiffness of photocrosslinked RGD-alginate gels regulates adipose progenitor cell behavior," *Biotechnol. Bioeng.*, vol. 108, no. 7, pp. 1683–1692, 2011.

[227] S. Hadjialirezaei, "Coating of alginate capsules," Norwegian University of Science and Technology, 2013.

[228] B. L. Strand, Y. a Mørch, T. Espevik, and G. Skjåk-Braek, "Visualization of alginate-poly-L-lysine-alginate microcapsules by confocal laser scanning microscopy," *Biotechnol. Bioeng.*, vol. 82, no. 4, pp. 386–94, 2003.

[229] X. Dong, C. Wei, T. Liu, and F. Lv, "Protoporphyrin incorporated alginate hydrogel: Preparation, characterization and fluorescence imaging in vivo," *RSC Adv.*, vol. 5, pp. 96336–96344, 2015.

[230] M. Huang, Z. Ma, E. Khor, and L. Y. Lim, "Uptake of FITC-chitosan nanoparticles by A549 cells," *Pharm. Res.*, vol. 19, no. 10, pp. 1488–1494, 2002.

APPENDICES

Appendix A: Pre-Extrusion Steps for Microsphere Synthesis

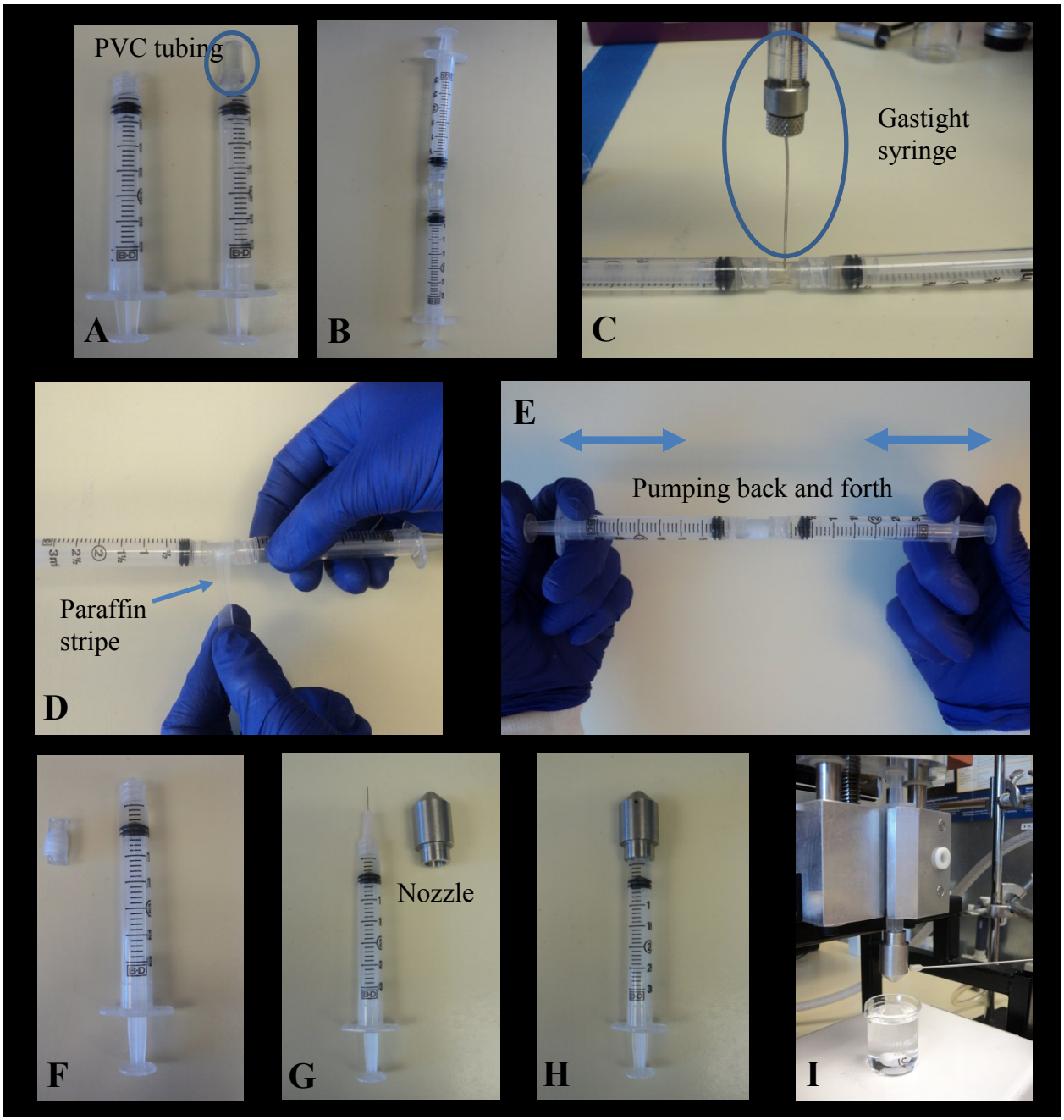

Figure A1. Illustration of the pre-extrusion steps for microsphere synthesis.

(A) Syringes (3 mL) containing the alginate with or without dextran sulfate (total of 300 µL polymer), with one syringe attached to the PVC tube (shown in the oval);
(B) Syringes connected by the PVC tubing;
(C) Injection of the activated simvastatin (100 µL) into the PVC tubing via the Gastight syringe (shown by the oval);

(D) Sealing of the injection site using 3-4 paraffin stripes;
(E) Mixing of the drug-polymer solution (400 μL) by pumping back and forth (for approximately three minutes) in order to obtain a homogenous solution ;
(F) Single syringe after transfer of the solution and detachment of the PVC tubing;
(G) Syringe with Luer Lock 30 gauge needle;
(H) Nozzle attached to the syringe;
(I) Clamped syringe on the extrusion pump.

Appendix B: Illustration of the Experimental Set-up for the Extrusion Process

Experimental set-up to analyze the effects of chitosan coating:

Extrusion Solution

- Simvastatin
- Alginate (conc. of 4% [w/v])

Gelation Medium

- 5% (w/v) $CaCl_2$
- With or without 0.1% (w/v) chitosan

Experimental set-up to analyze the effects of dextran sulfate:

Extrusion Solution

- Simvastatin
- Alginate (conc. of 4% [w/v])
- Dextran sulfate (conc. of 0.67, 2.0, or 3.35% [w/v])

Gelation Medium

- 5% (w/v) $CaCl_2$ with 0.1% (w/v) chitosan

Appendix C: Example of Calculation Tables for Simvastatin Preparation and Complexation with HP-βCD

Simvastatin Dissolution and Alkalization					
Preparation date	**MW (g/mol)**	**Lot #**	**Purity (%)**	**Volume of ethanol (µL)**	**Volume of 0.1N NaOH (µL)**
Sept 9th, 2014	418.6	0453431-7	100	100	150

Simvastatin pH Adjustments After Activation				
Recovered volume of simvastatin after the initial 2h incubation for activation (µL)	**Volume of 0.5 N HCl added (µL)**	**Total volume of simvastatin stock (µL)**	**Concentration of simvastatin stock (µM)**	**Final pH**
244	22	266	35923.54	4.25

Simvastatin Complexation with HP-βCD		
Displacement volume of HP-βCD powder when dissolved in simvastatin solution (µL)	**Total volume of simvastatin stock (µL)**	**Concentration of complexed simvastatin stock (µM)**
100	366	26108.36

Appendix D: Example of a Standard Curve Used to Measure the Concentration of Simvastatin Complexed with HP-βCD

Serial Dilution of Simvastatin Complexed with HP-βCD					
Vial	**Dilution factor of the source of simvastatin**	**Volume (µL) and source of simvastatin**	**Volume of diluent (µL)**	**Total volume (µL)**	**Final [simvastatin] (µM)**
A	261.08 of stock*	13 of stock	3381.1	3394.1	100
B	1.11 of vial A dilution	2700 of vial A dilution	300	3000	90
C	1.13 of vial B dilution	2400 of vial B dilution	300	2700	80
D	1.14 of vial C dilution	2100 of vial C dilution	300	2400	70
E	1.17 of vial D dilution	1800 of vial D dilution	300	2100	60
F	1.20 of vial E dilution	1500 of vial E dilution	300	1800	50
G	1.25 of vial F dilution	1200 of vial F dilution	300	1500	40
H	1.33 of vial G dilution	900 of vial G dilution	300	1200	30
I	1.50 of vial H dilution	600 of vial H dilution	300	900	20
J	2.00 of vial I dilution	400 of vial I dilution	400	800	10
K	2.00 of vial J dilution	300 of vial J dilution	300	600	5
L	NA	0	500	500	0

*Stock concentration of simvastatin = 26108.365 µM

The standard curve below, showing the UV absorbance at 238 nm of different concentrations of simvastatin complexed with HP-βCD (as shown in the above table), was generated on September 9th, 2014.